Vibrational Analysis of *all-trans*-Retinal

Bo Curry, Albert Broek,[1] Johan Lugtenburg,[1] and Richard Mathies*

Contribution from the Department of Chemistry, University of California, Berkeley, California 94720. *Received January 11, 1982*

Abstract: We have obtained Raman and IR spectra of *all-trans*-retinal and its 10-, 11-, 12-, and 15-monodeuterio, 11,12- and 10,11-dideuterio, and 19-trideuterio derivatives, as well as the 9- and 13-demethyl compounds. From these data, empirical assignments for most of the observed vibrations between 600 and 1700 cm^{-1} have been made. A modified Urey–Bradley force field, transferred from model polyenes and polyenals, has been refined to satisfactorily reproduce the frequencies and deuterium shifts observed in these spectra. From this analysis we have formulated a set of simple rules which describe the coupling between out-of-plane wagging vibrations of trans vinyl hydrogens and deuterons. In addition, the distribution of Raman intensity in the 1100–1400-cm^{-1} fingerprint region of the retinal spectrum is shown to result from vibrational mixing of the C_9 and C_{13} methyl stretches with the C–C stretches and CCH bends of the conjugated chain. The assignment of the observed spectral lines of retinal to specific vibrations and the formulation of a reliable force field provide a basis for predicting the effects of structural and environmental perturbations on the Raman spectrum of the retinylidene chromophore. Thus, we are now able to discuss the expected changes caused by Schiff base formation and by protonation of the Schiff base.

Introduction

The geometric isomers of retinal have considerable biological importance as chromophores in visual receptors and in bacteriorhodopsin, the light-driven proton pump of *Halobacterium halobium*.[2] Resonance Raman (RR)[3,4] spectra of these pigments have been used to determine the isomeric form of the chromophore[5] and the state of protonation of the Schiff base linkage between the chromophore and the protein.[6] However, much more information about chromophore structure and protein environment could be obtained from these RR spectra if all the observed lines could be assigned to specific vibrational modes. Previous workers have used RR spectra of chemically and isotopically modified pigment analogues and of model compounds to suggest preliminary vibrational assignments.[7-10] In our laboratory, spectra of visual pigments regenerated with deuterated retinals have been used to assign the prominent hydrogen out-of-plane (HOOP) vibrations of rhodopsin and its primary photoproduct, bathorhodopsin.[11-13] The further interpretation of these pigment spectra requires a more complete assignment of the observed lines, and the determination of the normal modes of vibration responsible for these lines. Such an assignment would be greatly facilitated if a vibrational analysis of the *all-trans*-retinal chromophore were available.

Early assignments of the preresonance Raman (PRR) spectrum of *all-trans*-retinal (I) were made by Rimai et al.[14] They pointed

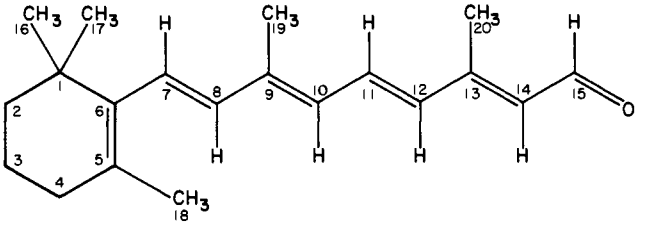

I

out that vibrations of the β-ionyl ring, because of their weak coupling with the conjugated π system, are unlikely to be observed in the PRR spectrum. They then classified the observed Raman lines as either "lattice modes" of the vinyl carbon skeleton or "group modes" associated with C=O, CH_3, or vinyl hydrogen motion. Lattice modes included the ~1575-cm^{-1} C=C stretch, and the observed vibrations in the 1100–1400-cm^{-1} "fingerprint" region, which they attributed to C—C stretching vibrations. CCH in-plane bends were noted to also occur in the 1100–1400-cm^{-1} range, but were not identified. Group vibrations were assigned to Raman lines at 1662 (C=O stretch), 1446 (CH_3 deformation), 1008 (C—CH_3 stretch), and 964-cm^{-1} (vinyl hydrogen out-of-plane wags). More recently, Cookingham et al. confirmed and extended these assignments with PRR spectra of demethyl, butyl-substituted, and ionone ring-modified retinals, as well as IR spectra of the unmodified retinals.[8b,15]

In the present work we have obtained PRR and IR spectra of *all-trans*-retinal and its 10-, 11-, 12-, and 15-monodeuterio, 11,12- and 10,11-dideuterio, 19-trideuterio, and 9- and 13-demethyl derivatives. We also present the results of a normal coordinate calculation which reproduces the observed frequency shifts of the major lines. The assignment of the out-of-plane hydrogen wags in the spectra of our retinal derivatives allows us to formulate general rules for the characteristic group frequencies of protonated and deuterated wags. With the help of our calculations we can also explain the major effects of the chain methyl groups on the

(1) Department of Chemistry, Leiden University, 2300 RA Leiden, The Netherlands.

(2) For general reviews see: (a) Birge, R. R. *Annu. Rev. Biophys. Bioeng.* **1981**, *10*, 315. (b) Ottolenghi, M. *Adv. Photochem.* **1980**, *12*, 97. (c) Stoeckenius, W.; Lozier, R. H.; Bogomolni, R. A. *Biochim. Biophys. Acta* **1979**, *505*, 215. (d) Honig, B. *Annu. Rev. Phys. Chem.* **1978**, *29*, 31. (e) Henderson, R. *Annu. Rev. Biophys. Bioeng.* **1977**, *6*, 87.

(3) Abbreviations used: RR, resonance Raman; PRR, preresonance Raman; HOOP, hydrogen out-of-plane; PSB, protonated Schiff base.

(4) For resonance Raman reviews see: (a) Mathies, R. *Chem. Biochem. Appl. Lasers* **1979**, *4*, 55. (b) Warshel, A. *Annu. Rev. Biophys. Bioeng.* **1977**, *6*, 273. (c) Callender, R.; Honig, B. *Ibid.* **1977**, *6*, 33.

(5) (a) Mathies, R.; Freedman, T. B.; Stryer, L. *J. Mol. Biol.* **1977**, *109*, 367. (b) Doukas, A. G.; Aton, B.; Callender, R. H.; Ebrey, T. G. *Biochemistry* **1978**, *17*, 2430. (c) Braiman, M.; Mathies, R. *Ibid.* **1980**, *19*, 5421.

(6) (a) Oseroff, A. R.; Callender, R. H. *Biochemistry* **1974**, *13*, 4243. (b) Lewis, A.; Spoonhower, J.; Bogomolni, R. A.; Lozier, R. H.; Stoeckenius, W. *Proc. Natl. Acad. Sci. U.S.A.* **1974**, *71*, 4462. (c) Terner, J.; Hsieh, C.-L.; Burns, A. R.; El-Sayed, M. A. *Biochemistry* **1979**, *18*, 3629. (d) Terner, J.; Hsieh, C.-L.; Burns, A. R.; El-Sayed, M. A. *Proc. Natl. Acad. Sci. U.S.A.* **1979**, *76*, 3046. (e) Ehrenberg, B.; Lemley, A. T.; Lewis, A.; v. Zastrow, M.; Crespi, H. L. *Biochim. Biophys. Acta* **1980**, *593*, 441. (f) Argade, P. V.; Rothschild, K. J.; Kawamoto, A. H.; Herzfeld, J.; Herlihy, W. C. *Proc. Natl. Acad. Sci. U.S.A.* **1981**, *78*, 1643.

(7) (a) Marcus, M. A.; Lewis, A.; Racker, E.; Crespi, H. *Biochem. Biophys. Res. Commun.* **1977**, *78*, 669. (b) Marcus, M. A.; Lewis, A. *Biochemistry* **1978**, *17*, 4722.

(8) (a) Cookingham, R.; Lewis, A. *J. Mol. Biol.* **1978**, *119*, 569. (b) Cookingham, R. E.; Lewis, A.; Lemley, A. T. *Biochemistry* **1978**, *17*, 4699. (c) Marcus, M. A.; Lemley, A. T.; Lewis, A. *J. Raman Spectrosc.* **1979**, *8*, 22.

(9) Stockburger, M.; Klusmann, W.; Gattermann, H.; Massig, G.; Peters, R. *Biochemistry* **1979**, *18*, 4886.

(10) Aton, B.; Doukas, A. G.; Narva, D.; Callender, R. H.; Dinur, U.; Honig, B. *Biophys. J.* **1980**, *29*, 79.

(11) Eyring, G.; Curry, B.; Mathies, R.; Fransen, R.; Palings, I.; Lugtenburg, J. *Biochemistry* **1980**, *19*, 2410.

(12) Eyring, G.; Curry, B.; Mathies, R.; Broek, A.; Lugtenburg, J. *J. Am. Chem. Soc.* **1980**, *102*, 5390.

(13) Eyring, G.; Curry, B.; Broek, A.; Lugtenburg, J.; Mathies, R. *Biochemistry* **1982**, *21*, 384.

(14) Rimai, L.; Gill, D.; Parsons, J. L. *J. Am. Chem. Soc.* **1971**, *93*, 1353.

(15) Cookingham, R. Ph.D. Thesis, Cornell University, Ithaca, NY, 1978.

0002-7863/82/1504-5274$01.25/0

Table I. Modified Urey-Bradley Force Field[a]

	coordinate	initial field[b]	refined field		coordinate	initial field[b]	refined field
chain stretches	$K(5=6)$	5.7	6.79	non-Urey-Bradley	h(CCH)(CCH)	0.06	0.08
	$K(7=8)$	5.7	6.20		h(C=CH)(CC-CH_3)	0.0	0.10
	$K(9=10)$	5.7	6.24		h(C-CH)(CC-CH_3)	0.0	0.14
	$K(11=12)$	5.7	6.44		h(CCC)(CCC)	0.172	−0.14
	$K(13=14)$	5.7	6.34		h(CCC)(CCH)	0.0	0.04
	$K(6-7)$	3.9	3.94	CH_3 group	K(CH)	4.741	4.741
	$K(8-9)$	3.9	4.30		H(CCH)	0.468	0.54
	$K(10-11)$	3.9	4.28		H(HCH)	0.50	0.464
	$K(12-13)$	3.9	4.09		F(CCH)	0.42	0.42
	$K(14-15)$	3.4	3.41		F(HCH)	0.11	0.11
	K(C-H)	4.73	4.73		h(HCH)(HCH)	−0.034	−0.078
	K(9-CH_3)	3.10	3.07	out-of-plane	w(7H)	0.475	0.466
	K(13-CH_3)	3.10	2.74		w(8H)	0.475	0.466
	K(C=O)	9.78	9.83		w(10H)	0.475	0.474
chain bends	H(CCC)	0.65	0.649		w(11H)	0.475	0.465
	H(C=CH)	0.326	0.316		w(12H)	0.475	0.466
	H(C-CH)	0.305	0.321		w(14H)	0.475	0.462
	H(CCO)	0.918	0.918		w(15H)	0.453	0.439
	H(CC-CH_3)	0.65	0.65		w(CH_3)	0.411	0.466
	H(OCH)	0.512	0.265		t(C-C)	0.19	0.19
Urey-Bradley	F(C=CH)	0.52	0.52		t(C=C)	0.54	0.55
	F(C-CH)	0.49	0.49		t(C-CH_3)[c]	0.137	0.137
	F(CC-CH_3)	0.49	0.49		$(6R,7H)_s$	−0.06	−0.06
	F(CCO)	0.46	0.46		$(8H,9CH_3)_s$	0.074	0.069
	F(OCH)	0.61	1.01		$(10H,11H)_s$	0.074	0.064
	F(CCC)	0.35	0.35		$(12H,13CH_3)_s$	0.074	0.061
non-Urey-Bradley	k(C=C)(C=O)	−0.661	−0.661		$(14H,15H)_s$	0.074	0.055
	k(C-C)(C=O)	0.30	0.43		$(5R,6R)_d$	0.181	0.173
	k(C=C)(C=C)	−0.472	−0.35		$(7H,8H)_d$	0.181	0.182
	$k(5=6)(7=8)$	−0.472	−0.09		$(9CH_3,10H)_d$	0.181	0.173
	k(C=C)(6-7)	0.30	0.05		$(11H,12H)_d$	0.181	0.166
	k(C=C)(C-C)	0.30	0.43		$(13CH_3,14H)_d$	0.181	0.182
	k(C-C)(C-C)	−0.09	−0.10		$(t,w)_d$	−0.278	−0.280
	k(CC)(C-CH_3)	0.8	0.5		$(t,w)_s$	−0.132	−0.118
					(t(C-CH_3),HCH)[c]	−0.02	−0.0318

[a] Stretching force constants (K, F, k) in mdyn/Å, bending constants in mdyn·Å/rad². Symbols used: K, diagonal stretch; H, diagonal bend; F, Urey-Bradley quadratic constant (linear term was set equal to −0.1 F); k, stretch-stretch interaction; h, bend-bend interaction (two common atoms); w, diagonal wag; t, chain torsion; $(w,w)_s$, wag-wag interaction across single bond; $(w,w)_d$, wag-wag interaction across double bond. [b] Details of the fit to model compounds are given in ref 23. [c] The bend-torsion interaction term was required because we defined t(C-CH_3) as a CCCH torsion rather than as a rigid rotation of the methyl group.

intensity pattern in the 1100–1400-cm^{-1} fingerprint region. A coherent picture emerges from this analysis which should be useful for understanding the spectra of the other retinal isomers, Schiff bases, and the retinal-containing pigments.

Experimental Section

All-trans deuterated retinal derivatives were synthesized using published methods[12,16] and were >95% isotopically and isomerically pure as shown by mass spectrometry, NMR, and high-performance liquid chromatography. The 15-deuterio retinal was prepared by reduction of *all-trans*-retinoic acid (Sigma) with $LiAlD_4$, followed by reoxidation to the aldehyde with MnO_2. The 9- and 13-demethylretinals were prepared by reduction of demethylretinoic acids with $LiAlH_4$ and reoxidation with MnO_2. Crystalline *all-trans*-retinal was purchased from Eastman and used without further purification.

Preresonance Raman spectra of the aldehydes were obtained in CCl_4 solution using 20–30- mW 676.4-nm excitation from a Spectra-Physics Model 171 krypton ion laser. Each spectrum is an average of three to five scans of stationary samples. No evidence of isomerization or sample degradation was observed in successive scans. The CCl_4 solvent peaks at 762 and 790 cm^{-1} were digitally subtracted, producing in some cases slight anomalies in this region. All labeled peaks in the spectra were clearly discernible before solvent subtraction. Spectral resolution is 4 cm^{-1} and peak positions are accurate to ±2 cm^{-1}.

IR spectra were obtained on thin films produced by dropwise evaporation of a pentane solution on a KBr window. Each spectrum is a single integration of 200 scans at 2-cm^{-1} resolution, taken on a Nicolet II FTIR spectrometer, and ratioed against a clean window. The absorbance spectra were manually digitized for final plotting with a Tektronix 4662 plotter. All peaks and shoulders in the digitized data were present in the original spectra, although the digitization process introduced minor distortions of line shapes. Reported peak positions are those of the original data, and are accurate to ±1 cm^{-1}.

Computational Methods. Normal mode calculations were performed using the Wilson FG method.[17] Force constants of a modified Urey–Bradley force field were chosen to best reproduce published vibrational assignments of butadiene,[18] acrolein,[19] hexatriene,[20] isoprene,[21] butene,[22] crotonaldehyde,[23] and their deuterated derivatives (Table I). The force constants used for in-plane polyene chain vibrations were slightly modified from those proposed by Inagaki et al.[24] Initial force constants for CH_3 group coordinates and for out-of-plane chain torsions and wags were taken from Levin et al.[22] and adapted for consistency with our Urey–Bradley field.

The calculations on *all-trans*-retinal were carried out on a model molecule in which C_1, C_4, and C_{18} were replaced by dummy "R" atoms, which have a mass of 15 and the potential parameters of saturated

(16) (a) Fransen, M. R.; Palings, I.; Lugtenburg, J.; Jansen, P. A. A.; Groenendijk, G. W. T. *Recl. Trav. Chim. Pays-Bas* **1980**, *99*, 384. (b) Broek, A. D.; Lugtenburg, J. *Ibid.* **1980**, *99*, 363. (c) Broek, A. D.; Lugtenburg, J. *Ibid.* **1982**, *101*, 102.

(17) Wilson, E. B.; Decius, J. C.; Cross, P. C. "Molecular Vibrations"; McGraw-Hill: New York, 1955; pp 54–65.

(18) (a) Panchenko, Y. N. *Spectrochim. Acta, Part A* **1975**, *31*, 1201. (b) Benedetti, E.; Aglietto, M.; Pucci, S.; Panchenko, Y. N.; Pentin, Y. A.; Nikitin, O. T. *J. Mol. Struct.* **1978**, *49*, 293.

(19) (a) Panchenko, Y. N.; Pulay, P.; Török, F. *J. Mol. Struct.* **1976**, *34*, 283. (b) Fukuyama, T.; Kuchitsu, K.; Morino, Y. *Bull. Chem. Soc. Jpn.* **1968**, *41*, 3021.

(20) Popov, E. M.; Kogan, G. A. *Opt. Spectrosc.* **1964**, *17*, 362.

(21) Tarasova, N. V.; Sverdlov, L. M. *Opt. Spectrosc.* **1966**, *21*, 176.

(22) Levin, I. W.; Pearce, R. A. R.; Harris, W. C. *J. Chem. Phys.* **1973**, *59*, 3048.

(23) Curry, B. Ph.D. Thesis, University of California, Berkeley, CA, in preparation.

(24) Inagaki, F.; Tasumi, M.; Miyazawa, T. *J. Raman Spectrosc.* **1975**, *3*, 335.

carbon. The masses of hydrogen and deuterium were taken as the "spectroscopic" masses (m_H = 1.088, m_D = 2.126) in order to simulate the effects of anharmonicity. The geometry of the model was taken as the equilibrium geometry calculated by Warshel's QCFF-π program[25] for the complete retinal molecule (see supplemental Table VIII), which for these purposes is not significantly different from the reported crystal geometry.[26] Methyl group orientation was chosen to be symmetrical with respect to reflection in the local plane of the conjugated chain. Test calculations were performed using QCFF-π in order to estimate the effects of omission of the β-ionyl ring. Calculated frequencies and normal modes for chain vibrations between C_7 and the aldehyde group were not significantly different for the model with the ring omitted. Also, because the retinal chain is nearly planar, the chain vibrations can be subdivided into motions primarily in the plane and those primarily out of the plane. This separation introduced errors of no more than 1 cm^{-1} in any frequency, with considerable savings of computation time.

The FG program was modified to generate its own standard basis set using the Fortran subroutine CHEMCO adapted from QCFF-π.[27] The chosen basis set includes all stretches and valence bends, and a nonredundant out-of-plane basis set consisting of one trans CCCC torsion for each chain bond, one trans CCCH torsion for each CH_3 group, and one Wilson-type out-of-plane wag[17] centered on each sp^2 carbon.

The initial force constants of Table I were refined to achieve the best least-squares fit to the observed Raman and IR frequencies of retinal and its deuterio derivatives. The usual refinement algorithms[28] first associate each experimental frequency ν_e with the nearest calculated frequency ν_c, and then minimize the sum of the squared residuals by adjusting the force constants. For a molecule the size of retinal, the density of normal modes is so high that the nearest frequency calculated with the unrefined force field is often not an appropriate assignment of the observed line. It is therefore necessary to incorporate empirical information about the character of the normal modes into the refinement algorithm.[29] We first assigned prominent C=C, C—C, CH_3, CCH bending, and HOOP vibrations based on observed frequency and intensity shifts in the Raman and IR spectra of the deuterio and demethyl derivatives. We then forced convergence to the chosen assignment by associating each ν_e with the calculated ν_c for which $|(\nu_e^2 - \nu_c^2)/\mathbf{a}_e \cdot \mathbf{a}_c|$ was smallest. When no "empirical" normal mode vector $\mathbf{a}_e$ could be deduced from the data, it was set equal to the calculated vector $\mathbf{a}_c$. The squared residuals were then minimized in the usual way. The final force constants of Table I were obtained by adjusting 30 in-plane parameters to fit 116 experimental frequencies (rms error <5 cm^{-1}), and 14 out-of-plane parameters to fit 34 frequencies (rms error <3 cm^{-1}). A more detailed description of the final force field can be found in supplemental Table IX.

Results and Discussion

The 141 fundamental frequencies of retinal can be separated into groups which are approximately vibrationally independent. Because the polyene chain is nearly planar, we will separately discuss the out-of-plane and the in-plane vibrations of the chain. The group vibrations of the chain methyl groups, although they are not all vibrationally isolated, are also conveniently discussed together. Finally, we have cataloged some of the vibrations attributable to the β-ionyl ring.

Out-of-Plane Chain Vibrations

The out-of-plane vibrations of the retinal chain can be classified as CCCC torsions or as wags of substituent hydrogens and methyl groups. The CCCC torsional modes and the out-of-plane wags of methyl carbons appear below 500 cm^{-1}, in a region of the spectrum masked by KBr absorption in the IR and by intense CCl_4 scattering in the Raman spectra. These modes were therefore not observed and will not be further discussed.

Hydrogen out-of-plane (HOOP) vibrations of linear polyenes, as we have previously discussed,[11] are observed between 750 and 1050 cm^{-1}, and they shift to 600–800 cm^{-1} when vinyl hydrogens are deuterated. This region of the PRR and IR spectra of *all-trans*-retinal and five vinyl-deuterated derivatives is presented in Figure 1. The most striking feature in this region of the retinal IR spectrum (Figure 1A) is the intense line at 966 cm^{-1}, which corresponds to a moderately intense, partially resolved, doublet in the Raman spectrum. This is a well-known IR group frequency associated with the in-phase ("A_u" in the local C_{2h} point group) HOOP vibration of trans ethylenic protons.[30] There are two such groups in retinal: $HC_7{=}C_8H$ and $HC_{11}{=}C_{12}H$. Upon deuteration at C_{11} or C_{12}, the $HC_{11}{=}C_{12}H$ component of the unresolved IR doublet should be removed. Our calculations (Table II) predict

Table II. Calculated HOOP Frequencies and Assignments for Retinal

	obsd	calcd	description[a]
unmodified		990	1.13(15w) – 0.49(14w)
	966	966	0.48(7w) + 0.59(8w) + 0.35(11w) + 0.41(12w)
	959	960	0.51(11w) + 0.52(12w) – 0.44(7w) – 0.43(8w)
	887	892	0.99(10w) – 0.66(11w)
	876	871	0.84(14w) + 0.47(12w) – 0.33(11w) – 0.33(10w)
		833	0.74(12w) – 0.58(11w) – 0.56(14w) + 0.33(7w) – 0.30(8w)
		815	0.84(7w) – 0.80(8w) + 0.33(10w)
10-D	962	963	0.66(7w) + 0.72(8w)
	956	955	0.70(11w) + 0.68(12w)
	878	876	0.76(14w) – 0.63(11w) + 0.58(12w)
		841	0.59(11w) – 0.63(12w) + 0.67(14w) – 0.32(10w)
		825	0.90(7w) – 0.84(8w)
	710	708	0.89(10w) – 0.27(12w) – 0.22($9CH_3$w)
11-D	964	964	0.65(7w) + 0.73(8w)
	917	920	0.85(12w) + 0.72(10w)
	880	877	0.78(10w) – 0.52(12w) – 0.51(14w)
		851	0.87(14w) – 0.46(12w)
		816	0.89(7w) – 0.84(8w) + 0.33(10w)
	740	741	0.92(11w) – 0.34(12w)
12-D	964	964	0.65(7w) + 0.73(8w)
	906	911	0.84(11w) + 0.51(10w)
	887	892	0.96(10w) – 0.71(11w)
	862	863	1.00(14w) + 0.23(15w)
		818	0.91(7w) – 0.86(8w) + 0.27(10w)
	722	726	0.94(12w) – 0.24($13CH_3$w)
11,12-D_2	964	964	0.65(7w) + 0.73(8w)
	890	896	1.09(10w) – 0.30(7w) – 0.20($9CH_3$w)
	864	864	1.01(14w) + 0.23(15w)
		818	0.91(7w) – 0.86(8w) + 0.26(10w)
	742	744	0.83(11w) – 0.62(12w) + 0.20($13CH_3$w)
	708	712	0.71(12w) + 0.39(11w) – 0.15($13CH_3$w)
10,11-D_2	963	963	0.66(7w) + 0.72(8w)
	908	905	1.04(12w) + 0.36(14w)
		854	0.96(14w) – 0.35(12w)
		827	0.93(7w) – 0.87(8w) + 0.21($9CH_3$w)
	762	759	0.85(11w) – 0.62(10w)
	692	690	0.69(10w) + 0.38(11w) – 0.31(12w) – 0.18($9CH_3$w)
15-D	967	966	0.46(7w) + 0.56(8w) + 0.37(11w) + 0.45(12w) + 0.30(10w)
	959	961	0.48(11w) + 0.51(12w) – 0.46(7w) – 0.46(8w)
	899	903	1.00(14w) – 0.57(15w) – 0.38(11w) + 0.22(12w)
		891	1.02(10w) – 0.55(11w)
		843	0.85(12w) – 0.65(11w)
		816	0.87(7w) – 0.83(8w) + 0.32(10w)
	801	798	0.69(15w) + 0.48(14w)

[a] Coefficients ($\partial S/\partial Q$) of hydrogen and CH_3 group out-of-plane wags (w) in the normal modes Q of *all-trans*-retinal. A positive wag coefficient represents hydrogen motion in the $+z$ direction. Those internal coordinates S contributing >10% to the potential energy are listed.

(25) Warshel, A.; Karplus, M. *J. Am. Chem. Soc.* **1974**, *96*, 5677.
(26) Hamanaka, T.; Mitsui, T.; Ashida, T.; Kakudo, M. *Acta Crystallogr., Sect. B* **1972**, *28*, 214.
(27) Warshel, A.; Karplus, M. *J. Am. Chem. Soc.* **1972**, *94*, 5612.
(28) Mann, D. E.; Shimanouchi, T.; Meal, J. H.; Fano, L. *J. Chem. Phys.* **1957**, *27*, 43.
(29) Peticolas, W. L.; Strommen, D. P.; Lakshminarayanan, V. *J. Chem. Phys.* **1980**, *73*, 4185.
(30) Potts, W. J.; Nyquist, R. A. *Spectrochim. Acta* **1959**, *15*, 679.

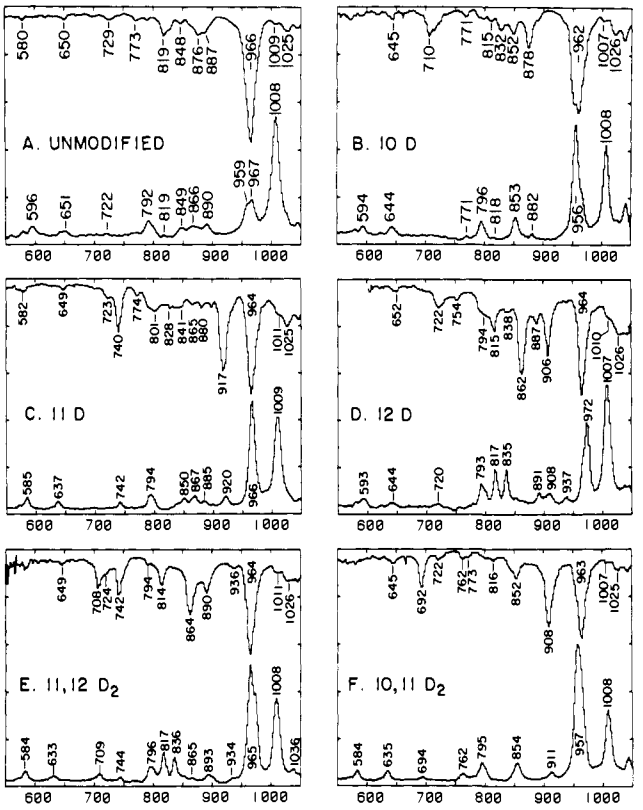

Figure 1. Raman and IR spectra of the 550–1050-cm^{-1} region of *all-trans*-retinal (A) and its 10-monodeuterio (B), 11-monodeuterio (C), 12-monodeuterio (D), 11,12-dideuterio (E), and 10,11-dideuterio (F) derivatives. The IR absorbance spectra are inverted to facilitate comparison.

that two new lines should appear: the deuterated wag in the 700–750-cm^{-1} range and the residual uncoupled H wag near 910 cm^{-1}. An unresolved lower frequency shoulder of the 966-cm^{-1} IR line, clearly apparent near 957 cm^{-1} in the original spectra, disappears in the 11-D and 12-D spectra (Figure 1C,D), and two new lines of moderate IR intensity appear at 740 and 917 cm^{-1} ([11-D]retinal) or at 722 and 906 cm^{-1} ([12-D]retinal), corresponding to weak Raman lines. When *both* C_{11} and C_{12} are deuterated (Figure 1E), the ~910-cm^{-1} line vanishes, and two deuterated modes appear at 708 and 742 cm^{-1}. The 959-cm^{-1} Raman line of unmodified retinal can thus be assigned to the HC_{11}=$C_{12}H$ A_u mode; the 920-cm^{-1} Raman line in [11-D]retinal and the 908-cm^{-1} line in [12-D]retinal are due to the 12-H and 11-H wags, respectively; and the weak Raman lines at 742 ([11-D]retinal) and 720 cm^{-1} ([12-D]retinal) are assigned to the 11-D and 12-D wags, respectively. The residual IR intensity at 964 cm^{-1} in the 11,12-D_2 spectrum is assigned to the other A_u HOOP arising from the HC_7=C_8H moiety.

Several points should be noted about these vibrations. *First*, the A_u modes of trans HRC=CRH groups, which are characteristic in IR spectra, usually appear weakly or not at all in PRR spectra, because only totally symmetric vibrations can be A-term enhanced.[31] A relative distortion of the planar geometry in either the ground or the resonant excited state, however, can cause these modes to appear strongly in the RR spectrum, as is observed in the spectra of the primary photoproducts of visual pigments[11] and bacteriorhodopsin.[32] The fact that the 959-cm^{-1} line in retinal also appears with moderate PRR intensity indicates that distortions along this coordinate occur upon excitation to its resonant excited electronic state.[33] *Second*, these assignments provide a good illustration of the complementary uses of Raman and IR spectra for vibrational assignments. The disappearance of the 959-cm^{-1} shoulder is obscured in the Raman spectra of [11-D]-, [12-D]-, and [11,12-D_2]retinal by the intense $CC_{11}D$ (966 cm^{-1}) and $CC_{12}D$ (972 cm^{-1}) in-plane rocks which shift down from the 1100–1400-cm^{-1} region in these derivatives. The pattern of shifts of the HOOP modes can be clearly discerned in the IR spectra, however, because the A_u HOOP modes are much more intense than are the in-plane rocks. *Third*, the two lines due to the $C_{11}H$ and $C_{12}H$ wags in the 11-D, 12-D, and 11,12-D_2 derivatives originate with two HOOP vibrations in the unmodified retinal: the 959-cm^{-1} "A_u" HOOP and an out-of-phase "B_g" HOOP at lower frequency.[11] This B_g vibration is expected to be weak in both IR and Raman spectra, and unlike the A_u HOOP it has a variable group frequency in the 750–850-cm^{-1} range.[34] For example, it appears weakly at 750 cm^{-1} in the Raman spectrum of *trans*-butene.[22] We calculate the HC_{11}=$C_{12}H$ B_g HOOP of retinal to appear at 833 cm^{-1}, but the observed shifts of the weak lines in this region of the 11-D, 12-D, and 11,12-D_2 spectra are not sufficiently distinctive to permit a definite assignment based on the disappearance of one of these lines. The HC_7=C_8H B_g HOOP is calculated to appear at 815 cm^{-1} but cannot be assigned to a particular line.

Few vibrational assignments for monodeuterated ethylene derivatives are available in the literature for comparison with our data. The prototype system, *trans*-stilbene, was studied in IR and Raman by Meic and Güsten.[35] Because crystalline *trans*-stilbene has an inversion center, the A_u HOOP is strictly forbidden in the Raman, while the B_g is forbidden in the IR. The authors assign the A_u HOOP to the very strong IR band at 963 cm^{-1}. Although they also attribute a very weak Raman line at 972 cm^{-1} to the B_g HOOP, we believe this assignment to be incorrect, since it lies well outside the expected frequency range for this vibration. In stilbene several weak depolarized Raman lines lie near 860 cm^{-1}, and one of these probably represents the B_g fundamental. In [α-D]stilbene the intense 963-cm^{-1} IR line shifts to 911 cm^{-1} with little loss of intensity, while a new weak line appears at 706 cm^{-1} in both IR and Raman spectra. This new 911-cm^{-1} line disappears in [α,α'-D_2]stilbene, and another weak line appears at 714 cm^{-1}. The similarity of these spectral shifts to those observed for retinal indicates that this pattern of deuterium shifts is a common feature of trans disubstituted ethylenic groups.

The assignment of the 10 and 14 HOOPs in retinal is less straightforward, both because of the low observed intensities of these lines and because there are few data available to establish characteristic frequencies. Potts and Nyquist[30] placed the wagging vibration of a hydrogen trans to a methyl group in the 800–840-cm^{-1} range for simple substituted ethylenes, with moderate IR intensity. Sverdlov et al.[34] assign this mode to the strong 808-cm^{-1} IR band of trimethylethylene, which corresponds to a weak Raman line. The absence of significant changes in our [10-D]retinal spectrum between 900 and 950 cm^{-1} requires that the 10 HOOP lie at a lower frequency. Comparison of the 10-D spectra (Figure 1B) with the unmodified spectra (Figure 1A) shows changes in the 848–890-cm^{-1} region, and a new IR line of moderate intensity at 710 cm^{-1}. The calculations in Table II predict the 10 HOOP to shift from 892 to 708 cm^{-1} in [10-D]-retinal. The 710-cm^{-1} IR line of 10-D can therefore be assigned to the 10-D wag, and the 10-H wag of unmodified retinal should be assigned to one of the weak lines observed between 848 and 890 cm^{-1}. The 14 HOOP is similarly calculated to lie at 871 cm^{-1}, and to shift to 863 cm^{-1} in the 12-D derivative (Table II). The strong IR line at 862 cm^{-1} in 12-D, which has little Raman intensity, is best assigned to the 14 HOOP shifted down from ~876 cm^{-1} with increased IR intensity. The constancy of this line in frequency and IR intensity in the 11,12-D_2 derivative argues that it is not the 10 HOOP. The large increase in intensity of

(31) Tang, J.; Albrecht, A. C. *Raman Spectrosc.* **1970**, *2*, 33.
(32) Braiman, M.; Mathies, R. *Proc. Natl. Acad. Sci. U.S.A.* **1982**, *79*, 403.
(33) The analogous situation has been discussed with reference to stilbene by Edelson, M.; Bree, A. *Chem. Phys. Lett.* **1976**, *41*, 562.
(34) Sverdlov, L. M.; Kovner, M. A.; Krainov, E. P. "Vibrational Spectra of Polyatomic Molecules"; Wiley: New York, 1974; pp 236–41, 249–69, 303–14.
(35) Meic, Z.; Güsten, H. *Spectrochim. Acta, Part A* **1978**, *34*, 101.

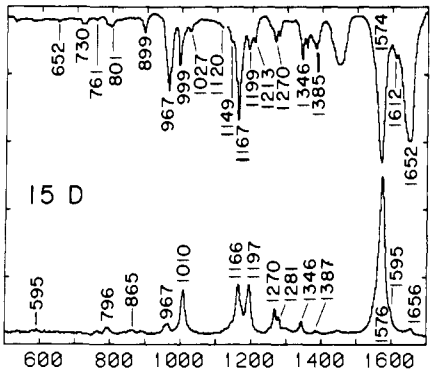

Figure 2. Raman and IR spectra of 15-monodeuterio *all-trans*-retinal.

the 14 HOOP in [12-D]retinal is consistent with the calculations, which predict a large reduction of mixing between the 12-H and 14-H wags upon 12-D substitution.

The HOOP vibration of the formyl hydrogen appears near 1000 cm^{-1} in model conjugated aldehydes (e.g., 1016 cm^{-1} in sorbaldehyde[23]), and our calculations predict the 15 HOOP to lie near 990 cm^{-1} in retinal. In [15-D]retinal (Figure 2) there is no significant loss of intensity near 1000 cm^{-1} which can be attributed to the 15 HOOP. Comparison with the calculations, however, suggests that the new weak IR line at 801 cm^{-1} is due to the shifted 15-D wag. The new IR band appearing at 899 cm^{-1} is best assigned to the 14 HOOP, which is calculated to shift from 871 to 903 cm^{-1} upon 15-D substitution (Table II).

A distinction should be made at this point between the extent to which two internal coordinates are *coupled* and the extent to which they are *mixed*. For simplicity, consider the two normal modes formed from the combination of two of the internal (basis) coordinates. The coupling between these basis coordinates depends on the magnitude of the off-diagonal term in the **FG** matrix. Such coupling terms occur either because of the nonorthogonality of the basis coordinates, which gives rise to off-diagonal elements in the **G** matrix (kinetic coupling), or because of off-diagonal force constants (potential coupling), or both. The normal modes formed from coupled basis coordinates will be shifted from their unperturbed frequencies (i.e., the frequencies they would have if the coupling were zero), and modification of one of the basis vibrations (e.g., by deuteration) will cause significant frequency shifts of both normal modes. Mixing, on the other hand, is a measure of the degree to which the basis coordinates exchange character in the normal modes. Strongly coupled internal coordinates will typically form strongly mixed normal modes. If the diagonal **FG** matrix elements of the two basis coordinates are nearly equal, however, they can mix significantly even if the off-diagonal elements of **FG** are small, and the normal modes will remain nearly degenerate. Such mixing allows the exchange of IR and Raman intensity, since the resulting normal modes have projections along both internal coordinates. In this case, modification of one of the basis coordinates will shift the frequency of only one of the normal modes, and the resulting vibrations will no longer be mixed because the near-degeneracy has been removed.

The degree to which substituents on adjacent carbon centers couple with each other, forming HOOP normal modes which are mixtures of the individual out-of-plane wags, depends both on the π-bond order of the CC bond joining the substituted centers and on the masses of the substituents. This is illustrated by a comparison of the 10-D, 11-D, and 12-D derivatives with the 11,12-D_2 and 10,11-D_2 derivatives. When two protons are trans to a double bond they couple strongly, forming A_u and B_g combinations widely separated in frequency. The drop of the A_u combination from 959 cm^{-1} in unsubstituted retinal to 917 or 906 cm^{-1} in the 11-D or 12-D derivatives is a measure of the extent of this coupling. When both the 11 and 12 centers are deuterated, however, the deuterated wags couple only weakly, since the observed lines in 11,12-D_2, at 742 and 708 cm^{-1}, have nearly the same frequencies and intensities as the corresponding wags in the monodeuterio derivatives (740 and 722 cm^{-1}, respectively). Our calculations (Table II) reproduce both the large splitting of the protonated wags and the much reduced coupling when C_{11} and C_{12} are deuterated. The situation is exactly reversed, however, for the C_{10} and C_{11} protons, which are trans to a single bond. When both are protonated, there is little coupling between the wags: the 959-cm^{-1} $HC_{11}{=}C_{12}H$ A_u HOOP drops by no more than 6 cm^{-1} in [10-D]retinal (Figure 1B). When both centers are deuterated they couple significantly across the single bond. In [10,11-D_2]-retinal (Figure 1F) two new IR lines are observed at 692 and 762 cm^{-1}, which correlate with weak Raman lines at 694 and 762 cm^{-1}. These lines are assigned to the 10-D and 11-D wags, respectively, since they are the only new lines in the 650–800-cm^{-1} region into which the deuterated HOOPs are expected to shift. Upon deuteration at C_{10}, therefore, the 11-D wag has shifted from 740 cm^{-1} in the 11-D derivative to 762 cm^{-1}, and lost most of its IR intensity. The 10-D wag similarly drops from 710 cm^{-1} in the 10-D derivative to 692 cm^{-1} in the 10,11-D_2 derivative. This splitting indicates a significant coupling of the deuterium wags across the single bond. The drop in IR intensity of the 762-cm^{-1} HOOP shows further that, in agreement with the calculations in Table II, the 10-D and 11-D HOOPs are strongly mixed, with the IR-active A_u combination at the *lower* frequency (692 cm^{-1}), instead of at the *higher* frequency as is observed for protons coupled across a double bond.

The dependence of the coupling between adjacent wags on mass and bond order can be understood by considering the potential and kinetic contributions to the energy. The vibrational problem in the Wilson FG method is formulated as

$$|\mathbf{FG} - \mathbf{E}| = 0$$

where **F** is the potential energy matrix, and **G** is the inverse kinetic energy matrix. In the simplified case where only two adjacent wags are considered, the problem becomes one of diagonalizing a 2 × 2 asymmetric **FG** matrix. The degree of coupling between the wags is determined by the magnitude of the off-diagonal matrix elements, while the symmetry of the higher frequency eigenvector is determined by their signs. An off-diagonal coupling term is given by

$$fg_{ij} = f_{ii}g_{ij} + f_{ij}g_{jj}$$

The g_{jj} element equals the inverse reduced mass, while the g_{ij} element is negative and independent of deuteration. The f_{ij} term, representing the potential energy coupling between the wags, is positive and nearly proportional to bond order, whereas the f_{ii} term is nearly independent of the bond order between the wags. The first term is thus negative and independent of either bond order or substituent mass, while the second term is positive and is smaller for deuterium substituents and for single bonds. The magnitudes of these elements are such that the net coupling term fg_{ij} is positive for protons across a double bond, nearly zero for deuterons across a double bond or for protons across a single bond, and negative for deuterons across a single bond.[36] This simple two-mode model can thus qualitatively explain the patterns observed for the 10-H, 11-H, and 12-H wags of retinal, and leads us to formulate the following general rules for HOOP frequencies in trans substituted polyene systems:

1. *Hydrogens trans to a double bond couple strongly ($fg_{ij} > 0$) forming an "A_u" HOOP in the 950–970-cm^{-1} range* which is strongly IR active, and a "B_g" HOOP from 750 to 850 cm^{-1} which is weak and poorly characterized. The 950–970-cm^{-1} IR group frequency is well known, and is nearly independent of the nature of any hydrocarbon substituents.[30] The observation of this line in its accustomed place in retinal ($\lambda_{max} \simeq 360$ nm), as well as in the protonated Schiff base of retinal ($\lambda_{max} \simeq 440$ nm) at 967 cm^{-1},[5a] shows that the increased delocalization of the double bonds does not significantly alter this frequency.

2. *A proton and a deuteron trans across a double bond give rise to two lines, one due to the largely uncoupled H wag (900–920*

(36) Typical values for retinal are: $f_{ii} = 0.465$, $f_{ij} = 0.170$ (double bond), $f_{ij} = 0.070$ (single bond), $g_{jj} = 1.353$ (H wag), $g_{jj} = 0.924$ (D wag), $g_{ij} = -0.274$. (Units of **F** are mdyn·Å/rad², units of **G** are rad²/Å²·dalton. Using these values gives $fg_{ij} = 0.103$ (double-bonded H), 0.030 (double-bonded D), −0.033 (single-bonded H), and −0.063 (single-bonded D.)

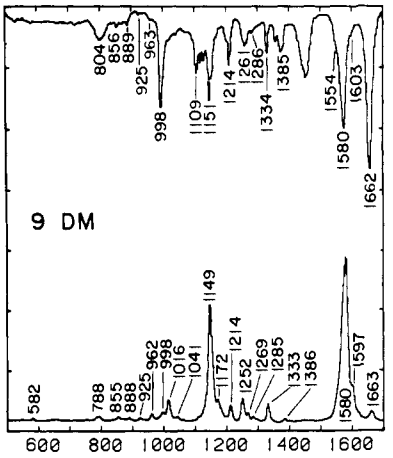

Figure 3. Raman and IR spectra of 9-demethyl-*all-trans*-retinal.

cm^{-1}) and the other due to the D wag (700–750 cm^{-1}). The data for *trans*-stilbene discussed above indicate that this shifting pattern is not unique to retinal, and that it does not depend upon the presence of adjacent protons. The RR spectra of [11-D]- and [12-D]isorhodopsin[13] demonstrate that this shifting pattern can also occur when the chromophore is embedded in a protein where it has a strongly red-shifted absorption maximum. It is interesting to note that the 11-cis chromophore of rhodopsin also conforms to this pattern: the native pigment has an intense RR line at 969 cm^{-1}, which shifts to 922 cm^{-1} in [11-D]rhodopsin and to 923 cm^{-1} in [12-D]rhodopsin.[13]

3. *Deuterons trans to a double bond couple weakly or not at all with each other ($fg_{ij} \simeq 0$). Deuterons trans to a single bond, on the other hand, couple more strongly than do protons, and the A_u symmetry combination lies at the lower frequency ($fg_{ij} < 0$).* This pattern of "single bond" coupling is also observed for the 10-H and 11-H protons of bathorhodopsin, which couple only slightly when both are protonated, but split by 37 cm^{-1} when deuterated.[13] These data have been used to show that bathorhodopsin contains a C_{10}–C_{11} single bond with a bond order not greatly different from that of *all-trans*-retinal. The observed coupling between adjacent hydrogen wags can thus provide the means for *experimental* estimation of individual bond orders in retinal-containing pigments.

4. *A proton trans to a CH_3 group across a double bond appears between 850 and 900 cm^{-1}. When deuterated, it appears near 700 cm^{-1}.* Our calculations predict that, if identical force constants are used, the kinetic coupling with the adjacent CH_3 group out-of-plane wag gives an isolated frequency near 890 cm^{-1}, ~20 cm^{-1} lower than that for a proton trans to a deuteron (Table II). The assignment of 10-H and 14-H HOOPs in the 850–890-cm^{-1} region of *all-trans*-retinal is consistent with the unambiguous assignment of the intense RR lines at 875 and 854 cm^{-1} in bathorhodopsin to the 10-H and 14-H wags, respectively.[13]

The spectra of 9- and 13-demethylretinal illustrate the coupling of adjacent A_u HOOPs across single bonds. In 9-demethylretinal, the $HC_7{=}C_8H$, $HC_9{=}C_{10}H$, and $HC_{11}{=}C_{12}H$ A_u HOOPs can couple with one another to produce an evenly spaced triplet of normal modes. The calculations (Table III) predict the in-phase (relative A_u HOOP phases + + +) combination to lie at 998 cm^{-1}, the (+ 0 −) combination at 960 cm^{-1}, and the combination with two nodes (+ − +) at 923 cm^{-1}. These predicted frequencies are in good agreement with the observed weak Raman lines at 998, 962, and 925 cm^{-1} (Figure 3), split by 36 cm^{-1}. As expected, the in-phase combination at 998 cm^{-1} exhibits most of the IR intensity. In 13-demethylretinal there are two adjacent unsubstituted double bonds, the $HC_{11}{=}C_{12}H$ and the $HC_{13}{=}C_{14}H$. The two corresponding A_u HOOPs are split by 42 cm^{-1}, giving rise to an IR-active in-phase combination at 984 cm^{-1} and a weak out-of-phase combination at 942 cm^{-1} (Figure 4), in agreement with the calculated values of 984 and 941 cm^{-1} (Table IV). The $HC_7{=}C_8H$ A_u HOOP remains isolated at 967 cm^{-1}. The agreement between observed and calculated A_u HOOP frequencies in the demethyl derivatives provides further confirmation that wag–wag coupling across single bonds is correctly modeled by our force field.

Table III. Frequencies and Assignments for 9-Demethylretinal[a]

	obsd	calcd	description
in-plane	1663	1664	0.36(C=O) + 0.55(15H) − 0.11(14–15)
	1580	1581	0.24(11=12) + 0.20(7=8) + 0.57(11H) − 0.52(12H) − 0.13(8–9) − 0.15(10–11) − 0.11(12–13)
		1572	0.25(9=10) − 0.21(13=14) + 0.50(10H) − 0.49(9H) − 0.11(10–11) + 0.14(12–13) + 0.10(14–15)
		1553	0.27(13=14) + 0.20(9=10) + 0.58(14H) − 0.13(14–15)
	1333	1332	0.58(14H) + 0.14(12–13) − 0.19(13–CH_3)
	1268	1268	0.52(11H) + 0.16(9=10) + 0.14(11=12)
	1252	1261	0.52(11H) + 0.57(12H) − 0.57(7H) − 0.50(8H) + 0.12(12–13)
	1214	1217	0.20(12–13) − 0.10(10–11) + 0.53(14H)
	1172	1161	0.28(10–11)
	1149	1141	0.23(8–9) + 0.09(6–7) + 0.08(10–11)
	1016	1017	0.69(20CH_3r) + 0.14(12–13)
		874	0.25(13–CH_3)
HOOP	998	998	0.49(9w) + 0.46(10w) + 0.34(7w) + 0.40(8w) + 0.29(11w) + 0.25(12w)
		990	1.13(15w) − 0.48(14w)
	962	960	0.47(7w) + 0.46(8w) − 0.48(11w) − 0.50(12w)
	925	923	0.38(7w) + 0.29(8w) − 0.44(9w) − 0.53(10w) + 0.38(11w) + 0.43(12w)
		882	0.72(11w) − 0.60(12w) − 0.55(14w) + 0.36(9w) − 0.52(10w)
		855	0.81(14w) + 0.50(9w) − 0.46(10w)
		824	0.73(7w) − 0.76(8w) − 0.40(11w) + 0.45(12w)
		789	0.55(7w) − 0.34(8w) − 0.55(9w) + 0.59(10w) + 0.28(11w) − 0.47(12w)

[a] Symbols used: H, in-plane hydrogen rock; w, out-of-plane wag; r, CH_3 in-plane rock. The in-plane hydrogen rocks are defined as linear combinations of the two valence bends involving the rocking hydrogen (e.g., $11H \equiv 1/\sqrt{2}(C_{10}C_{11}H - C_{12}C_{11}H)$. The in-plane and out-of-plane methyl rocks are defined as in ref 22. Only the more prominent lines and those discussed in the text are given.

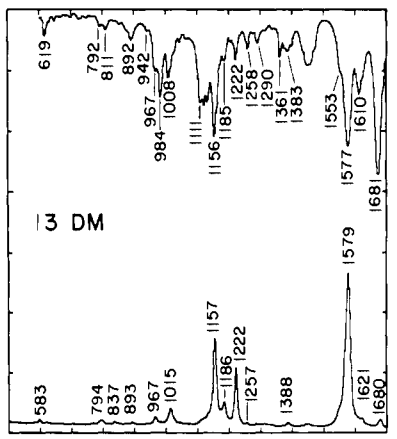

Figure 4. Raman and IR spectra of 13-demethyl-*all-trans*-retinal.

In-Plane Chain Vibrations

The in-plane vibrations of the retinal chain can be classified into groups which are relatively isolated in frequency. The five C=C stretches and the C=O stretch appear between 1500 and 1700 cm^{-1}. The fingerprint region from 1100 to 1400 cm^{-1} contains C–C stretches and CCH in-plane bends mixed in com-

Table IV. Frequencies and Assignments of 13-Demethylretinal[a]

	obsd	calcd	description
in-plane	1680	1661	0.36(C=O) + 0.57(15H) − 0.12(14−15)
	1610	1609	0.39(5=6) − 0.18(6−7)
	1579	1579	0.26(11=12) + 0.15(7=8) + 0.15(9=10) + 0.65(11H) − 0.52(12H) − 0.12(8−9) − 0.18(10−11) − 0.11(12−13)
		1316	0.56(11H) + 0.23(8−9) − 0.17(9−CH_3)
	1290	1298	0.66(14H) − 0.77(12H) + 0.11(11=12)
	1257	1270	0.44(11H) − 0.52(14H) + 0.14(11=12) + 0.14(13=14)
		1228	0.70(13H) + 0.56(14H)
	1222	1203	0.13(8−9) + 0.48(8H) + 0.49(10H) + 0.51(11H) + 0.44(12H)
	1186	1176	0.26(10−11) − 0.11(12−13) + 0.46(10H)
	1157	1141	0.28(12−13) + 0.12(10−11)
	1015	1019	0.69(19CH_3r) + 0.13(8−9)
		885	0.24(9−CH_3)
HOOP		995	1.03(15w) + 0.44(13w)
	984	984	0.40(11w) + 0.44(12w) + 0.35(13w) + 0.59(14w) − 0.50(15w)
	967	964	0.65(7w) + 0.72(8w)
	942	941	0.45(11w) + 0.45(12w) − 0.46(13w) − 0.52(14w) + 0.30(10w)
	892	891	1.00(10w) − 0.65(11w)
		849	0.90(12w) − 0.59(11w) − 0.42(13w) + 0.22(14w)
		816	0.87(7w) − 0.83(8w) + 0.33(10w)
		770	0.73(13w) − 0.78(14w) − 0.36(11w) + 0.21(12w) − 0.21(15w)

[a] See footnotes to Table III.

binations which are strongly dependent on chain configuration. Finally, the skeletal CCC and $CCCH_3$ bending modes are calculated to lie below 700 cm^{-1} and to involve a small degree of in-plane hydrogen motion, and thus to be slightly sensitive to chain deuteration. On this basis the two weak Raman lines at 596 and 651 cm^{-1} (Figure 1A), which shift by ~10 cm^{-1} in the deuterated derivatives, are assigned to CCC bends.

Double-Bond Stretches. The C=O stretch has been assigned to the Raman line at 1663 cm^{-1},[14] and the intense IR absorption at 1660 cm^{-1} in Figure 5 fully confirms this assignment. The drop of the frequency of this line to 1656 cm^{-1} in [15-D]retinal (Figure 2) agrees well with the calculated drop from 1664 to 1651 cm^{-1} due to coupling with the $C_{15}H$ in-plane rock. Note that this line shows a weak solvent dependence, appearing at 1663 cm^{-1} in CCl_4 solution, 1660 cm^{-1} in the amorphous thin film, and 1654 cm^{-1} in the crystal.[37]

In our solution Raman and thin-film IR spectra (Figure 5) only three lines can be observed between 1500 and 1650 cm^{-1} which could be assigned to the five C=C fundamentals: the weak IR band at 1611 cm^{-1}, the rather broad intense Raman and IR line at 1577 cm^{-1}, and a weak shoulder near 1550 cm^{-1}. In the crystal Raman spectrum, however, five lines in this region are resolved, at 1547, 1568, 1594, 1611, and 1634 cm^{-1}.[37] Because the C=C stretches incorporate significant contributions of CCH in-plane rocking motion of bonded hydrogens, these lines are expected to be sensitive to vinyl deuteration. First, note that the intense Raman line at 1577 cm^{-1} shifts only slightly to 1574 cm^{-1} in the 10-D derivative (Figure 5B), although it is significantly narrowed, and the 1554-cm^{-1} shoulder becomes much more prominent. In the 11-D and 12-D derivatives, however, this intense line splits into a doublet near 1555 and 1567 cm^{-1} (Figure 5C,D), while in the 11,12-D_2 derivative the doublet appears at 1536 and 1567 cm^{-1} (Figure 5E). In the 10,11-D_2 derivative a single broad line is observed at 1556 cm^{-1} (Figure 5F). We conclude that the 1577-cm^{-1} line of the unmodified compound is in reality composed of two nearly degenerate, unresolved lines near 1577 and 1567

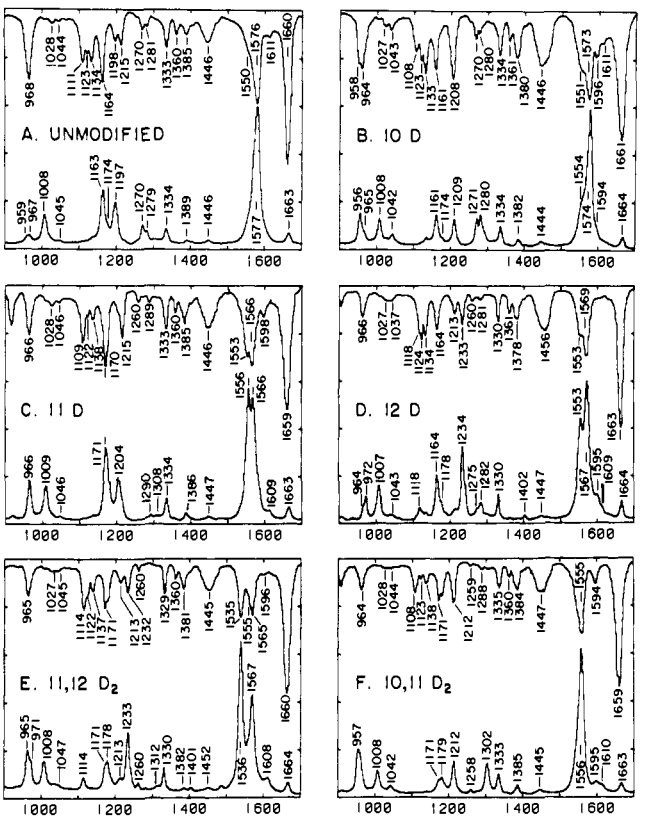

Figure 5. Raman and IR spectra of the 900–1700-cm^{-1} region of *all-trans*-retinal (A) and its 10-monodeuterio (B), 11-monodeuterio (C), 12-monodeuterio (D), 11,12-dideuterio (E), and 10,11-dideuterio (F) derivatives.

cm^{-1}, and that the 1577-cm^{-1} component downshifts by ~20 cm^{-1} upon C_{11} or C_{12} deuteration and by 40 cm^{-1} when both are deuterated. The 1567-cm^{-1} component, on the other hand, is relatively insensitive to C_{11} or C_{12} deuteration, but shifts to ~1550 cm^{-1} when C_{10} is deuterated. The decreased line widths of the 1567-cm^{-1} line of 11,12-D_2 and of the 1574-cm^{-1} line of 10-D support this placement of two unresolved lines near 1577 cm^{-1}. Deconvolution of the 1577-cm^{-1} band using the methods of Sundius[38] gives the best fit to three bands at 1578, 1569, and 1550 cm^{-1}, with relative integrated intensities of 1.0, 0.37, and 0.10, respectively, each having a line width of ~15 cm^{-1}. The calculations in Table V predict the C_{11}=C_{12} stretch to downshift by ~22 cm^{-1} upon deuteration of either the 11 or 12 position and by 45 cm^{-1} when both positions are deuterated, while the C_9=C_{10} stretch remains nearly constant. The intense line at 1577 cm^{-1} in the unmodified compound can therefore be assigned to the C_{11}=C_{12} stretch, which shifts to 1574 cm^{-1} in 10-D, to 1556 cm^{-1} in 11-D and 10,11-D_2, to 1553 cm^{-1} in 12-D, and to 1536 cm^{-1} in 11,12-D_2 retinals. The observation that the effects on the C_{11}=C_{12} stretch frequency of deuteration at the 11 and 12 positions are nearly equal and additive indicates that the $C_{11}H$ and $C_{12}H$ rocks contribute equally to this normal mode, as predicted by the calculations (Table V). The C_9=C_{10} stretch is predicted to be sensitive to 10-D substitution, downshifting from 1572 cm^{-1} in the unmodified retinal to 1547 cm^{-1} in 10-D, while the C_{11}=C_{12} stretch remains virtually unchanged in frequency. The unresolved shoulder near 1569 cm^{-1} in unmodified retinal, the 1554-cm^{-1} Raman shoulder in [10-D]retinal, and the more intense resolved lines at 1567 cm^{-1} in the 11-D, 12-D, and 11,12-D_2 derivatives can thus be assigned to the C_9=C_{10} stretching vibration. The fact that the C_{11}=C_{12} and C_9=C_{10} stretches alone account for over 90% of the PRR intensity in the ethylenic region indicates that the bond-order changes upon electronic excitation of retinal are largely concentrated in the region of these two double bonds.

(37) Cookingham, R. E.; Lewis, A.; Collins, D. W.; Marcus, M. A. *J. Am. Chem. Soc.* **1976**, *98*, 2759.

(38) Sundius, T. *J. Raman Spectrosc.* **1973**, *1*, 471.

Table V. Frequencies and Assignments of C=C Stretches for Retinal[a]

	obsd	calcd	description
unmodified	1611	1609	0.39(5=6) − 0.17(6−7)
	1594	1596	0.28(7=8) − 0.19(11=12) + 0.55(7H) − 0.63(8H) − 0.15(6−7) − 0.15(8−9)
	1577	1580	0.27(11=12) + 0.17(7=8) + 0.61(11H) − 0.59(12H) − 0.11(8−9) − 0.16(10−11) − 0.13(12−13)
	1568	1572	0.27(9=10) − 0.19(13=14) + 0.54(10H) − 0.09(8−9) − 0.13(10−11) + 0.12(12−13) + 0.09(14−15)
	1550	1555	0.28(13=14) + 0.19(9=10) + 0.60(14H) − 0.33(15H) − 0.14(14−15)
10-D	1611	1609	0.39(5=6) − 0.17(6−7)
	1596	1596	0.29(7=8) − 0.17(11=12) + 0.56(7H) − 0.66(8H) − 0.15(6−7) − 0.16(8−9)
	1574	1578	0.27(11=12) + 0.18(7=8) + 0.50(11H) − 0.66(12H) − 0.10(6−7) − 0.08(10−11) − 0.17(12−13)
		1561	0.29(13=14) − 0.14(9=10) − 0.13(11=12) + 0.61(14H) − 0.34(15H) + 0.14(10−11) − 0.14(14−15)
	1551	1547	0.32(9=10) + 0.15(13=14) + 0.36(10D) + 0.31(14H) − 0.11(8−9) − 0.14(10−11)
11-D	1609	1609	0.39(5=6) − 0.18(6−7)
	1598	1594	0.32(7=8) + 0.62(7H) − 0.72(8H) − 0.17(6−7) − 0.18(8−9)
	1566	1573	0.22(9=10) − 0.14(11=12) − 0.20(13=14) + 0.37(10H) − 0.48(12H) − 0.38(14H) + 0.16(12−13) + 0.09(14−15)
	1556	1559	0.23(11=12) + 0.24(9=10) + 0.63(10H) − 0.38(11D) + 0.55(12H) − 0.10(8−9) − 0.21(10−11) − 0.12(12−13)
		1553	0.27(13=14) − 0.20(11=12) + 0.11(9=10) + 0.59(14H) − 0.30(15H) − 0.14(14−15)
12-D	1609	1609	0.39(5=6) − 0.18(6−7)
	1595	1593	0.33(7=8) + 0.64(7H) − 0.71(8H) − 0.17(6−7) − 0.17(8−9)
	1567	1574	0.28(9=10) − 0.14(13=14) + 0.12(11=12) + 0.67(10H) − 0.49(11H) − 0.30(14H) − 0.12(8−9) − 0.20(10−11)
	1553	1556	0.32(11=12) − 0.13(9=10) + 0.11(7=8) + 0.57(11H) − 0.43(12D) − 0.08(10−11) − 0.17(12−13)
		1554	0.31(13=14) + 0.16(9=10) + 0.64(14H) − 0.36(15H) − 0.11(12−13) − 0.15(14−15)
11,12-D_2	1608	1609	0.39(5=6) − 0.18(6−7)
	1596	1593	0.33(7=8) + 0.65(7H) − 0.74(8H) − 0.18(6−7) − 0.18(8−9)
	1567	1569	0.29(9=10) − 0.18(13=14) + 0.59(10H) − 0.36(14H) − 0.10(8−9) − 0.15(10−11) + 0.10(12−13) + 0.08(14−15)
	1555	1554	0.29(13=14) + 0.18(9=10) + 0.62(14H) − 0.34(15H) − 0.08(12−13) − 0.14(14−15)
	1536	1535	0.36(11=12) + 0.46(11D) − 0.47(12D) − 0.36(10H) − 0.18(10−11) − 0.18(12−13)
10,11-D_2	1610	1609	0.39(5=6) − 0.17(6−7)
	1595	1594	0.32(7=8) + 0.62(7H) − 0.72(8H) − 0.17(6−7) − 0.18(8−9)
		1571	0.20(11=12) + 0.22(13=14) − 0.14(9=10) + 0.61(12H) + 0.41(14H) − 0.28(15H) − 0.19(12−13) − 0.10(14−15)
	1556	1553	0.26(13=14) − 0.22(11=12) + 0.58(14H) − 0.29(15H) + 0.07(10−11) − 0.13(14−15)
	1544	1542	0.31(9=10) + 0.17(11=12) + 0.42(10D) − 0.32(11D) + 0.40(12H) − 0.12(8−9) − 0.22(10−11) − 0.07(12−13)

[a] All internal coordinates contributing >10% to the potential energy of the normal mode are included. Coefficients of CC stretches, because of their greater reduced mass, are $\sim 1/\sqrt{6}$ of CCH rocking coefficients having comparable potential energy contributions.

Because the C=C stretching lines are due to normal modes involving primarily motion of adjacent conjugated carbon atoms, it would be expected that they would have kinetic and potential energy interactions with each other. The frequency shift of each line upon deuteration at the other bond is a measure of the strength of the coupling between them, and this coupling is quite weak (e.g., the 1577 → 1574 cm^{-1} shift of the $C_{11}=C_{12}$ stretch in 10-D, and the ~1569 → 1567 cm^{-1} shift of the $C_9=C_{10}$ stretch in 11-D and 12-D). It is therefore possible to describe these C=C stretching normal modes as primarily localized stretches of individual double bonds. The variation of intensity among the C=C stretching modes in the derivatives indicates that some mixing of mode character occurs in either the ground or the excited state, however, which is expected for nearly degenerate lines even if the interaction constants are quite small.

The remaining three fundamentals due to the $C_5=C_6$, $C_7=C_8$, and $C_{13}=C_{14}$ stretches cannot be so readily assigned from our data, both because of their low intensity and because none of these carbon atoms was substituted. Our calculations predict these stretches to appear between 1550 and 1620 cm^{-1} and to be insensitive to deuteration at C_{10}, C_{11}, C_{12}, or C_{15}. Three resolved lines appear in the crystal Raman spectrum at 1547, 1594, and 1611 cm^{-1},[37] and lines appear within 3 cm^{-1} of 1594 and 1611 cm^{-1}, with varying intensity, in the IR and/or Raman spectra of all of our derivatives (Figures 5A–F). The 1551-cm^{-1} line is masked by the intense $C_9=C_{10}$ or $C_{11}=C_{12}$ stretch in all of the derivatives except 11,12-D_2, 15-D, and unmodified retinal, in which it appears as a weak shoulder. The spectra of retinal analogues with truncated conjugated chains can help to empirically distinguish the $C_{13}=C_{14}$ stretch from the two C=C stretches near the β-ionyl ring. The PRR spectrum of β-ionone shows two strong lines at 1591 and 1605 cm^{-1}, which must be due to the $C_5=C_6$ and $C_7=C_8$ stretches.[8b,23] Also, the IR and PRR spectra of all-trans "C_{18}-ketone", in which C_{14} is replaced by a carbonyl oxygen, show C=C stretching lines at 1571, 1591, and 1601 (sh) cm^{-1},[23] with the shoulder observed at 1550 cm^{-1} in retinal conspicuously absent. This suggests that the 1611- and 1594-cm^{-1} lines of retinal should be assigned to the $C_5=C_6$ and $C_7=C_8$ stretches, while the 1550-cm^{-1} shoulder is due to the $C_{13}=C_{14}$ stretch. The relatively constant frequency of the ~1595- and ~1605-cm^{-1} lines in these model compounds, which differ in the length of their conjugated chains, is consistent with the assignment of these lines to the $C_5=C_6$ and $C_7=C_8$ stretches, since the twist of the chain about the C_6—C_7 bond[26] is likely to make these double-bond stretching frequencies less sensitive to increased π-electron delocalization. The analogous weak lines observed at 1580 and 1599 cm^{-1} in light-adapted bacteriorhodopsin are also probably due to the $C_5=C_6$ and $C_7=C_8$ stretches.[5c]

Fingerprint C–C Stretches. The fingerprint C–C stretches and CCH rocks are considerably mixed with each other, so that characterization of a normal mode as a localized rock or stretch is only approximate, although sometimes convenient. Because the character of the normal modes varies in the derivatives, it is often more useful to describe the effects of deuteration as the increase or withdrawal of a particular component of a normal mode, resulting in a frequency shift, rather than as a shift of a

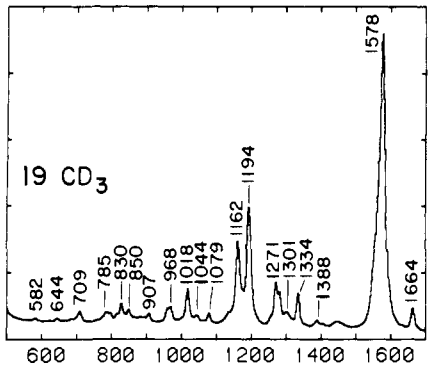

Figure 6. Raman spectrum of 19-trideuterio-*all-trans*-retinal.

substantially unchanged vibration. Also, because these modes derive their Raman intensity from admixtures of C—C and C=C stretches,[39] which may be minor components of the normal mode, considerable intensity variation can occur even for normal modes whose major rocking components remain the same.

As noted by Rimai,[14] the C–C stretches should appear with intensity in both IR and Raman spectra, while the CCH bends are expected to be weak in both. In extended long-chain polyenes the C–C stretches are delocalized along the chain, and only the lowest frequency, totally symmetric stretch combination appears intensely near 1140 cm^{-1} (e.g., 1138 cm^{-1} in diphenyltetradecaheptaene[40]). In retinal, however, this simple vibrational pattern is altered by the interaction of the methyl groups on C_9 and C_{13} with the adjacent C_8–C_9 and C_{12}–C_{13} stretches. The strong interaction of the C–CH_3 stretches with the adjacent C—C and C=C stretches is almost entirely kinetic in origin and will occur for any reasonable force field. Its effect is to raise the C–C stretching vibration by ~80 cm^{-1}, while lowering the C–CH_3 stretch by approximately the same amount. For example, the effect of substituting a CH_3 group onto a conjugated single bond is well illustrated by comparing butadiene, which has C–C stretch at 1205 and CCH rock at 1279 cm^{-1},[18] with isoprene, whose C–C stretch and CCH rock shift up to 1289 and 1300 cm^{-1} when mixed with the C–CH_3 stretch at 953 cm^{-1}.[21] In retinal, as will be discussed below, the increased frequency of the C_8–C_9 and C_{12}–C_{13} stretches, caused by mixing with the adjacent C–CH_3 stretches, raises them to a frequency range where they mix more strongly with CCH rocks (1200–1350 cm^{-1}). The Raman spectrum of retinal therefore has a more complex fingerprint than that of unsubstituted polyenes, as suggested by Stockburger et al.,[9] because the intrinsic intensity of the C–C stretches is distributed among more than a single line.

We begin by assigning the intense IR and Raman line at 1163 cm^{-1} to the C_{10}–C_{11} stretch for the following reasons. First, this is the only C–C bond of the chain which has an environment similar to that of a long unsubstituted polyene, and should therefore exhibit a "normal" frequency near 1160 cm^{-1}. Second, the Raman line at 1163 cm^{-1} is insensitive to deuteration at C_{10}, C_{12}, or C_{19} (Figures 5B,5D,6), but increases to 1171 cm^{-1} in the 11-D derivative (Figure 5C) and to ~1178 cm^{-1} in the 11,12-D_2 and 10,11-D_2 (Figure 5E,F). Our calculations (Table VI) predict the C_{10}–C_{11} stretch to couple weakly with the $C_{11}H$ rock, and to shift up by 8 cm^{-1} when C_{11} is deuterated. The C_{10}–C_{11} stretch is calculated to couple less with the $C_{10}H$ rock, which lies at higher frequency than the $C_{11}H$ rock (see below), and also to be uncoupled from the more distant $C_{12}H$ rock. Therefore, the C_{10}–C_{11} stretch should be nearly unaffected by deuteration at C_{10} and C_{12}, as observed. Third, the C_{10}–C_{11} stretch should be sensitive to the configuration of the adjacent double bonds. The 13-cis retinal isomer has a line near 1163 cm^{-1}, while the 9-cis and 11-cis isomers do not have lines at this frequency.[8b]

Although the frequency of the C_{10}–C_{11} stretch is insensitive to deuteration at C_{10} or C_{12}, the IR and especially the Raman intensity of this line decreases in the 10-D, 12-D, 10,11-D_2, and 11,12-D_2 derivatives. The drop in IR intensity can qualitatively be attributed to a decrease of the contribution of the C_{10}–C_{11} stretch coordinate to this normal mode in the deuterated derivatives (see Table VI). However, the calculated decrease in C_{10}–C_{11} stretch character is insufficient to explain the ~four-fold decrease of relative intensity observed in the Raman spectrum of the 10,11-D_2 derivative. Preresonance Raman intensity depends on the character of both the ground- and excited-state normal modes. Because the reduction of intensity of the ~1163-cm^{-1} line in the derivatives is more marked in the Raman spectra than in the IR spectra, it is likely that deuteration also changes this normal mode in the excited state.

The C_8–C_9 and C_{12}–C_{13} stretches are expected to lie at higher frequency than the C_{10}–C_{11} stretch, because of their coupling with the adjacent methyl stretches. Two moderately intense IR bands are observed in the expected frequency range in unmodified retinal (Figure 5A), at 1198 and 1215 cm^{-1}, corresponding to an intense line and a weaker shoulder in the Raman spectrum. These lines can be assigned to the C_8–C_9 and C_{12}–C_{13} stretches on the basis of their sensitivity to deuteration. Both of these stretches are calculated to couple only slightly with the $C_{11}H$ rock (Table VI), in agreement with the observation that the 1197-cm^{-1} line shifts up by only 7 cm^{-1} in the 11-D derivative, while the 1215-cm^{-1} line is unshifted (Figure 5C). In [12-D]- and [11,12-D_2]retinal (Figure 5D,E) the 1197-cm^{-1} line vanishes, and an intense Raman line appears at 1233 cm^{-1}, while a weak Raman line remains at 1213 cm^{-1}. The C_{12}–C_{13} stretch is calculated to be moderately coupled with the $C_{12}H$ rock, and to shift up from 1214 to 1229 cm^{-1} when C_{12} is deuterated. The simplest interpretation is that the C_{12}–C_{13} stretch appears at 1197 cm^{-1} in unmodified retinal and shifts to 1233 cm^{-1} in the 12-D and 11,12-D_2 derivatives, retaining its Raman intensity. The C_8–C_9 stretch, which should couple less strongly with the $C_{12}H$ rock, can then be assigned to the weak Raman line at 1213 cm^{-1} in these derivatives. In the 10-D and 10,11-D_2 derivatives, moderately intense IR and Raman lines are observed at ~1210 cm^{-1}, while Raman intensity migrates up to ~1280 cm^{-1} (10-D) or to 1302 cm^{-1} (10,11-D_2). The C_8–C_9 stretch is calculated to be strongly coupled with the $C_{10}H$ rock, and to shift up to ~1290 cm^{-1} in 10-D and 10,11-D_2, where it mixes with the remaining hydrogen rocks. These rocks could then borrow intensity from the shifted C_8–C_9 stretch, contributing to the general increase in Raman intensity in this region. The residual line at 1209 cm^{-1} in the 10-D derivative and at 1212 cm^{-1} in 10,11-D_2 can then confidently be assigned to the C_{12}–C_{13} stretch.

Comparison with the calculated frequencies in Table VI shows that the above assignments are in reasonable agreement with the calculations. However, the calculation places the C_8–C_9 stretch at lower frequency than the C_{12}–C_{13} stretch in the unmodified compound. This calculated ordering is insensitive to the choice of force constants within reasonable limits, and we were unable to reverse the calculated assignments without introducing substantial errors in the deuterium shifts. It is, therefore, also possible that in unmodified retinal the suggested assignment should be reversed, placing the C_8–C_9 stretch at 1197 cm^{-1} and the C_{12}–C_{13} stretch at 1215 cm^{-1}. In this case, changes in the mixing between these two stretches, in either the ground state or the excited state, could account for the variations in relative PRR intensity in the deuterated derivatives. The calculated mixing of these stretches to form a symmetric combination at 1229 cm^{-1}, for example, could explain the large Raman intensity of the 1234-cm^{-1} line in the 12-D derivative.

The 9- and 13-demethyl derivatives in Figures 3 and 4 further demonstrate the effect of the methyl groups on the C–C chain stretches. Removal of either CH_3 group causes a downshift of the adjacent C–C stretch (because it is no longer coupled with the C–CH_3 stretch), which then can interact more strongly with the conjugated C_{10}–C_{11} stretch at 1163 cm^{-1}. This interaction causes the symmetric combination of the adjacent C–C stretches to shift downward and increase in intensity (Tables III, IV). In the 9-demethyl derivative, the intense 1197-cm^{-1} line disappears, while a line remains at 1214 cm^{-1}. Our calculations predict the

(39) Rimai, L.; Heyde, M. E.; Gill, D. *J. Am. Chem. Soc.* **1973**, *95*, 4493.
(40) Margulies, L.; Stockburger, M. *J. Raman Spectrosc.* **1979**, *8*, 26.

Table VI. Frequencies and Assignments of the Retinal Fingerprint

	obsd	calcd	description[a]
unmodified		1377	0.40(10H) − 0.55(15H) − 0.33(12H) + CH_3 sym def
		1360	0.81(15H) + 0.54(10H) + 0.14(9−CH_3)
	1334	1339	0.79(14H) + 0.56(15H) + 0.12(12−13) − 0.20(13−CH_3)
		1312	0.52(8H) + 0.45(11H) + 0.22(8−9) − 0.16(9−CH_3) − 0.11(6−7)
		1287	0.93(7H) − 0.30(8H) + 0.17(7=8)
	1279	1280	0.63(12H) − 0.48(11H) + 0.16(11=12)
	1270	1261	0.67(11H) − 0.59(8H) + 0.47(12H) + 0.13(12−13)
	1215	1214	0.21(12−13) − 0.10(10−11) + 0.65(14H) + 0.28(12H) − 0.11(13−CH_3)
	1197	1203	0.15(8−9) + 0.61(10H) + 0.50(8H) + 0.43(11H) + 0.37(12H)
	1174	1173	0.11(6−7) + 0.18(10−11) + 0.36(10H)
	1163	1164	0.22(10−11) − 0.10(6−7) + 0.23(11H)
	1111	1115	0.33(14−15)
10-D		1372	0.91(15H) + 0.33(12H) − 0.33(14H)
	1334	1342	0.78(14H) + 0.70(15H) − 0.37(12H) + 0.10(12−13) − 0.17(13−CH_3)
		1322	0.69(8H) + 0.45(7H) + 0.14(10−11) − 0.10(12−13) + 0.11(13−CH_3)
	1286	1305	0.27(8−9) − 0.25(9−CH_3)
		1286	0.89(7H) − 0.35(8H) + 0.17(7=8) + 0.10(8−9)
	1280	1275	0.59(12H) − 0.56(11H) + 0.17(11=12)
	1271	1259	0.62(11H) + 0.62(12H) − 0.45(8H) + 0.15(12−13) − 0.12(13−CH_3)
	1209	1212	0.19(12−13) + 0.65(14H) + 0.44(12H) + 0.34(11H)
	1174	1180	0.12(6−7) + 0.16(10−11) + 0.46(8H)
	1161	1163	0.19(10−11) − 0.12(6−7) + 0.30(11H)
	1108	1115	0.33(14−15)
	956	956	0.50(10D) + 0.12(8−9)
11-D		1376	0.48(10H) − 0.58(15H) − 0.32(12H) + CH_3 sym def
		1360	0.84(15H) + 0.52(10H) + 0.13(9−CH_3)
	1334	1337	0.82(14H) + 0.50(15H) + 0.14(12−13) − 0.21(13−CH_3)
	1308	1305	0.61(8H) + 0.23(8−9) − 0.13(6−7) − 0.18(9−CH_3)
	1290	1287	0.96(7H) + 0.17(7=8)
	1260	1264	0.79(12H) + 0.12(11=12) − 0.40(8H)
	1215	1223	0.17(12−13) − 0.14(10−11) + 0.47(14H) + 0.41(8H) + 0.37(12H)
	1204	1209	0.13(8−9) − 0.14(12−13) + 0.55(10H) + 0.44(8H)
	1171	1172	0.25(10−11) + 0.47(10H)
		1171	0.17(6−7)
	1109	1115	0.33(14−15)
	966	959	0.81(11D) + 0.07(10−11)
12-D		1371	0.74(15H) − 0.46(10H)
		1360	0.57(10H) + 0.76(15H) − 0.34(8H) + 0.14(9−CH_3)
	1330	1330	0.87(14H) + 0.44(15H) + 0.10(13=14) + 0.10(12−13) − 0.22(13−CH_3)
		1311	0.52(8H) + 0.40(11H) + 0.22(8−9) − 0.11(6−7) − 0.16(9−CH_3)
	1282	1287	0.94(7H) + 0.17(7=8)
	1275	1263	0.85(11H) − 0.49(8H) − 0.35(7H) + 0.10(11=12)
12-D	1234	1229	0.17(12−13) + 0.11(8−9) + 0.47(10H) + 0.42(14H)
	1213	1208	0.10(8−9) − 0.16(12−13) + 0.57(10H) − 0.44(14H)
	1178	1181	0.23(10−11) + 0.10(6−7)
	1164	1165	0.16(10−11) − 0.12(6−7)
	1118	1119	0.33(14−15)
	972	980	0.54(12D) + 0.16(13−CH_3)
11,12-D_2		1370	0.74(15H) − 0.50(10H)
		1360	0.56(10H) + 0.78(15H) + 0.14(9−CH_3)
	1330	1328	0.89(14H) + 0.40(15H) + 0.12(13=14) + 0.12(12−13) − 0.23(13−CH_3)
	1312	1305	0.62(8H) + 0.23(8−9) − 0.13(6−7) − 0.17(9−CH_3)
		1287	0.97(7H) + 0.17(7=8)
	1233	1235	0.19(12−13) + 0.11(8−9) + 0.59(8H) + 0.37(14H)
	1213	1208	0.11(8−9) − 0.15(12−13) + 0.59(10H) − 0.42(14H)
	1178	1182	0.25(10−11) + 0.34(10H)
	1171	1170	0.15(6−7)
	1114	1118	0.32(14−15)
	971	981	0.60(12D) + 0.32(11D) + 0.15(13−CH_3)
	965	956	0.78(11D) + 0.07(10−11)
10,11-D_2		1369	0.97(15H) + 0.10(13=14)
	1333	1339	0.83(14H) + 0.61(15H) + 0.12(12−13) − 0.19(13-CH_3)
		1317	0.74(8H) + 0.52(7H) + 0.15(10−11) + 0.10(6−7)
	1302	1303	0.26(8−9) + 0.10(9=10) + 0.37(8H) − 0.23(9−CH_3)
	1288	1286	0.90(7H) + 0.10(8−9) − 0.17(7=8)
	1258	1259	0.85(12H) + 0.13(11=12) + 0.13(12−13) − 0.12(13−CH_3)
	1212	1221	0.18(12−13) − 0.13(10−11) + 0.51(14H)
	1179	1189	0.18(10−11) + 0.11(12−13) + 0.43(12H) − 0.41(8H)
	1171	1171	0.15(6−7)
	1108	1115	0.33(14−15)
	965	959	0.36(10D) + 0.58(11D) + 0.10(8−9)
	957	949	0.55(11D) − 0.35(10D) + 0.10(10−11)
15-D		1372	0.64(10H) − 0.37(12H) + 0.39(14H) + 0.11(9−CH_3)
	1346	1344	0.75(14H) − 0.32(10H) − 0.34(12H) + 0.10(13=14) + 0.10(12−13) − 0.20(13−CH_3)
		1312	0.51(8H) + 0.44(11H) + 0.22(8−9) − 0.11(6−7) − 0.16(9−CH_3)
		1287	0.93(7H) + 0.17(7=8)
	1281	1280	0.64(12H) − 0.47(11H) + 0.16(11=12)
	1270	1262	0.66(11H) − 0.59(8H) + 0.43(12H) + 0.14(12−13)
	1213	1218	0.21(12−13) − 0.10(10−11) + 0.58(14H) − 0.11(13−CH_3)
	1197	1203	0.15(8−9) + 0.60(10H) + 0.44(11H) + 0.38(12H) + 0.50(8H)
		1173	0.11(6−7) + 0.18(10−11) + 0.35(10H)
	1166	1164	0.22(10−11) − 0.10(6−7) + 0.23(11H)
	1149	1145	0.30(14−15) + 0.53(15D)
	999	991	0.78(15D) + 0.13(14−15)

[a] All internal coordinates contributing >10% to the potential energy of the normal mode are included. Coefficients of CC stretches, because of their greater reduced mass, are $\sim 1/\sqrt{6}$ of CCH rocking coefficients having comparable potential energy contributions.

downshift of the C_8–C_9 stretch in 9-demethylretinal, where it mixes with the C_{10}–C_{11} stretch to produce modes at 1141 and 1161 cm^{-1}, with the symmetric combination at the lower frequency. These correspond to the observed lines at 1149 and 1172 cm^{-1} in Figure 3. The C_{12}–C_{13} stretch is calculated to shift only slightly, and can be assigned to the 1214-cm^{-1} line. In the 13-demethyl derivative (Table IV) the symmetric and asymmetric combinations of the C_{10}–C_{11} and C_{12}–C_{13} stretches are calculated to lie at 1141 and 1176 cm^{-1}, respectively. We therefore assign the observed 1157- and 1186-cm^{-1} lines of 13-demethylretinal to the mixed C_{12}–C_{13} and C_{10}–C_{11} stretches. The 1222-cm^{-1} line is best assigned to the residual C_8–C_9 stretch. Removal of both chain methyl groups causes a collapse of the fingerprint intensity into a single intense line at 1148 cm^{-1} (in *trans*-didemethylretinoic acid[41]) characteristic of unsubstituted polyenes.

The C—C stretch α to the C=O group appears only weakly in the Raman spectra of model conjugated aldehydes, but it absorbs strongly in the IR. Although this stretch appears at 1152 cm^{-1} in neat crotonaldehyde, it drops to 1123 cm^{-1} in sorbaldehyde, where it gives a strong IR band which shifts to 1151 cm^{-1} in [1-D]sorbaldehyde.[23] We therefore expect the corresponding stretch in retinal to appear at lower frequency than the intense C_{10}–C_{11} stretch, to be readily observed in the IR spectrum but weak in the Raman spectrum, and to be sensitive to deuteration at C_{15}. The 1111-cm^{-1} band in our retinal IR spectra is insensitive to 10-D or 11-D substitution, but increases to 1118 cm^{-1} in 12-D, and to 1149 cm^{-1} in 15-D (Figures 2, 5). The 1111-cm^{-1} IR line can therefore be assigned to the C_{14}–C_{15} stretch. A small degree of coupling between this stretch and the nearby C_{10}–C_{11} stretch at 1163 cm^{-1} would then be responsible for the ~3 cm^{-1} upshift of the C_{10}–C_{11} stretch in [15-D]retinal. The considerable reduction of the C_{14}–C_{15} force constant below that of the other single bonds (Table I), which was required in order to fit this frequency in the calculations, is consistent with the lower π-bond order of the C_{14}–C_{15} bond predicted in QCFF-π calculations of retinal. This assignment was also suggested by Cookingham et al.,[8b] who observed a line near 1111 cm^{-1} in the 9-cis, 11-cis, and 13-cis isomers of retinal whose intensity increases as the cis bend approaches the CHO terminal group.

Finally, we attribute the 1174-cm^{-1} shoulder in the *all-trans*-retinal spectrum to the remaining conjugated C_6–C_7 single bond stretch, because it increases dramatically in Raman intensity in 3,4-dehydroretinal.[8b] Such an increase of Raman intensity is expected as a result of the extension of the conjugated π system into the ring. The remaining IR lines at 1123 and 1134 cm^{-1} are attributed to vibrations of the β-ionyl ring, as discussed below.

Fingerprint CCH Bends. Vinyl deuteration of the retinal chain will cause the corresponding CCH bend (or "rock") to shift out of the fingerprint region. Thus the 1270-cm^{-1} line of unmodified retinal consists largely of $C_{11}H$ rocking motion, since this line vanishes whenever the 11 position is deuterated (11-D, 10,11-D_2, 11,12-D_2). No major lines above 1200 cm^{-1} are observed to vanish in the 10-D, 12-D, or 15-D derivatives, which indicates that the normal modes which have predominantly $C_{10}H$, $C_{12}H$, and $C_{15}H$ character do not have much intensity. The direction of the shifts of other fingerprint lines in these derivatives, however, can be used to deduce an allowable frequency range for the unsubstituted weak vibrations, when it is recognized that coupling of these vibrations causes the coupled normal modes to split *apart*. The 1334-cm^{-1} line, for example, is unaffected by 10-D or 11-D substitution (Figure 5B,C,F) but shifts down to 1330 cm^{-1} in 12-D and up to 1346 cm^{-1} in [15-D]retinal. This suggests that this line can be assigned to the $C_{14}H$ rock, which is calculated to be mixed with the $C_{15}H$ rock and more weakly with the $C_{12}H$ rock. The fact that it shifts *up* in 15-D and *down* in 12-D indicates that the unseen $C_{15}H$ rock is at *higher* frequency, and the $C_{12}H$ rock at *lower* frequency, than 1334 cm^{-1}. The high frequency of the $C_{14}H$ rock can be attributed to coupling with the C_{12}–C_{13} stretch and with the C_{13}–CH_3 stretch, as predicted by the calculations (Table VI). Mixing with the C_{13}=C_{14} stretch may also contribute Raman intensity to this mode. The disappearance of this line in 13-demethylretinal (Figure 4) is then naturally attributable to the removal of the C_{13}–CH_3 stretch interaction, and the resulting drop of the C_{12}–C_{13} stretch frequency. The upshift of the intense C_{12}–C_{13} stretch to 1234 cm^{-1} in [12-D]retinal (Figure 5D) shows both that this stretch contains a significant contribution from the $C_{12}H$ rocking motion, and also that the unseen $C_{12}H$ rock is *above* 1234 cm^{-1} in unmodified retinal. The $C_{12}H$ rocking mode, although it cannot be assigned to any observed vibration, can thus nonetheless be confidently placed between 1234 and 1330 cm^{-1}. One possibility consistent with our calculations is that the $C_{12}H$ rock lies at 1279 cm^{-1} in the unmodified retinal spectrum, where it derives intensity by mixing with the $C_{11}H$ rock at 1270 cm^{-1}, and with the C_{11}=C_{12} stretch.

Our calculations predict the $C_{10}H$ rock, which is similar to the $C_{14}H$ rock in being trans to a methyl group, to lie slightly above the $C_{14}H$ rock at 1334 cm^{-1}. No lines in this region of the 10-D and 10,11-D_2 derivatives are observed to vanish (Figure 2B,F). The shift of the C_8–C_9 stretch to ~1280 cm^{-1} in 10-D, however, confirms that the unseen $C_{10}H$ rock of unmodified retinal lies at least above 1280 cm^{-1}.

When deuterium is substituted for hydrogen, the corresponding rock is shifted out of the fingerprint region to near 970 cm^{-1}, where it appears largely unmixed with other rocking vibrations. The strong new Raman lines appearing at 956 cm^{-1} in the 10-D, at 966 cm^{-1} in the 11-D, and at 972 cm^{-1} in the 12-D derivative (Figure 5B–F) must represent these deuterium rocks, which derive Raman intensity by mixing with C–C stretches. These rocks apparently do not couple with each other when they are deuterated, since they appear as unsplit degenerate lines in the 10,11-D_2 and 11,12-D_2 derivatives. The new intense IR band at 999 cm^{-1} in [15-D]retinal (Figure 2) is similarly assigned to the $C_{15}D$ rock, which borrows intensity through mixing with the C_{14}–C_{15} stretch. The high frequency of this line is consistent with the placement of the $C_{15}H$ rock near 1360 cm^{-1} in unmodified retinal.

Methyl Group Vibrations

Besides their profound effects on the retinal fingerprint, the chain methyl groups contribute their own group vibrations to the retinal spectra. The HCH bending vibrations form three combinations, a symmetric and two degenerate asymmetric deformations, which give reliable IR group frequencies at ~1380 and ~1445 cm^{-1}, respectively, corresponding to weak Raman lines.[34] The "in-plane" CCH methyl rock appears in model compounds between 1000 and 1100 cm^{-1}, weakly in the IR and with variable Raman intensity, while the "out-of-plane" methyl rock, which is not coupled with fingerprint vibrations, appears at a slightly higher frequency.[34] The C–CH_3 methyl stretching mode is quite variable in both frequency and intensity, because of its strong interaction with CC stretches and CCH rocks involving motion of the methyl-substituted carbon atom. Lines from 800 cm^{-1} in isobutene[42] to 953 cm^{-1} in isoprene[21] have been assigned to this vibrational mode.

The amorphous band near 1446 cm^{-1} in the IR spectrum therefore includes contributions from the HCH deformations of all five CH_3 groups, as well as CH_2 scissors vibrations of the ring, which also have characteristic IR frequencies in this region.[34] The 1360-, 1385-cm^{-1} IR doublet is characteristic of *gem*-dimethyl symmetric deformations, and was thus attributed to the methyl groups on C_1.[8b] The remaining IR intensity near 1385 cm^{-1} and the majority of the Raman intensity near 1389 cm^{-1} is then probably due to symmetric deformations of the three CH_3 groups attached to the conjugated chain. These vibrations are calculated to appear at ~1385 cm^{-1}, and are expected to exhibit greater Raman intensity than deformations of methyl groups attached to the ring.

The strong 1008-cm^{-1} Raman line clearly represents a coupled vibration involving motion of *both* chain methyl groups, since it shifts upward by 7–10 cm^{-1} in [19-CD_3]retinal and in both 9- and 13-demethylretinal (Figures 3, 4, 6). The fact that modifications

(41) Freedman, T. B.; Mathies, R.; Stryer, L., unpublished results.

(42) Harris, W. C.; Levin, I. W. *J. Mol. Spectrosc.* **1971**, *39*, 441.

of either methyl group shift this line upward by an approximately equal amount implies that the uncoupled CH_3 vibrations are nearly degenerate at ~1016 cm^{-1} and that they couple to form normal modes that are split apart by ~8 cm^{-1}. Because the 1008-cm^{-1} line exhibits nearly all of the Raman intensity, it must represent the symmetric combination of the two methyl modes. The antisymmetric combination would then lie near 1024 cm^{-1}, with nearly zero intensity. These arguments apply with equal validity whether the coupled vibrations are methyl stretches or methyl rocks.

The large Raman intensity of the 1008-cm^{-1} line is apparently due to mixing with the C–C stretches of the conjugated chain. The C–CH_3 stretches and CH_3 rocks themselves are expected to participate only slightly in the resonant π–π^* electronic transition and will therefore have little intrinsic PRR intensity. This requirement that the vibration responsible for the 1008-cm^{-1} line be mixed with C–C stretches precludes this mode being the out-of-plane methyl rock, which could not mix effectively with chain stretches. It must therefore be an in-phase combination of either the C–CH_3 stretches or the CH_3 in-plane rocks of the two chain methyl groups.

Comparison of our deuterated retinal spectra (Figure 1) with the calculated CH_3 vibrational frequencies (Table VII) strongly suggests that the 1008-cm^{-1} line is the methyl rock. First, this frequency is more consistent with a methyl rock assignment. The C–CH_3 stretches of model compounds lie between 800 and 960 cm^{-1} (e.g., 953 cm^{-1} in isoprene), while CH_3 rocks have been assigned from 963 cm^{-1} in propylene to as high as 1146 cm^{-1} in *trans*-butene.[21,22,34] Second, our force constant set consistently places the methyl stretches 50–100 cm^{-1} below the methyl rocks, while correctly reproducing the interactions of the methyl stretches with the chain C–C stretches and CCH rocks. Third, when the chain carbons adjacent to the methyl groups are deuterated, the C–CH_3 stretches are calculated to couple kinetically much more strongly with the CCD vinyl bends than are the methyl rocks. For example, the C_9–CH_3 and C_{13}–CH_3 stretches are calculated to shift from 888 and 871 cm^{-1} to 884 and 825 cm^{-1} when C_{12} is deuterated. These shifts are even greater when the calculated methyl stretch frequencies are forced to be closer to that of the $C_{12}D$ (e.g., at 1008 cm^{-1}). Although the antisymmetric combination of the two rocks is also calculated to shift up by ~10 cm^{-1} in the 12-D derivative, the lower frequency combination shifts up by no more than 3 cm^{-1}, and should retain its Raman intensity (Table VII). The remarkable constancy of the 1008-cm^{-1} line not only in our vinyl-deuterated derivatives, but also in other retinal isomers,[8b] in their PSB's,[5a] in the retinal-containing pigments,[4] and in other carotenoids[43] seems therefore inconsistent with a methyl stretch assignment. The methyl rock, on the other hand, is calculated to be much more localized, and is thus expected to be much less sensitive to the configuration and environment of the molecule.

The C–CH_3 stretches cannot lie near 960 cm^{-1} submerged beneath the A_u HOOPs, or they would be observed to couple strongly with the adjacent vinyl deuterated rocks, producing a split pair of lines centered near 960 cm^{-1}. Yet the $C_{10}D$ and $C_{12}D$ rocks appear at 956 and 972 cm^{-1}, nearly identical with the $C_{11}D$ rock (966 cm^{-1}) which is unperturbed by C–CH_3 stretches. Nor can the C–CH_3 stretches lie between 890 and 950 cm^{-1}, since there are no Raman lines in this region, and it is improbable that the intensity of the methyl stretches is zero. It therefore appears likely that these stretches contribute to the cluster of weak Raman lines between 849 and 890 cm^{-1} (Figure 1A), which is well within the normal range of such vibrations in model molecules. In [10-D]retinal, Raman intensity is lost in the 866–890-cm^{-1} region, apparently shifting to 853 cm^{-1}, and in [12-D]retinal the 866-cm^{-1} line apparently shifts to 835 or 817 cm^{-1} (Figure 1B,D). These shifts agree well with the calculated shifts of C–CH_3 stretches in these derivatives.

The Raman spectrum of [19-CD_3]retinal (Figure 6) is consistent with these assignments. The new line appearing at 1079 cm^{-1} is assigned to the $C_{19}D_3$ symmetric deformation shifted down from ~1390 cm^{-1}, based on its calculated deuterium shift of 1388 → 1110 cm^{-1} (Table VII). The shift of the 1008-cm^{-1} line to 1018 cm^{-1} is due to the removal of one of the degenerate methyl rocks, and therefore represents the upshifted residual $C_{20}H_3$ rock. The in-plane $C_{19}H_3$ rock is calculated to shift from ~1015 to 850 cm^{-1}, while the C_9–CH_3 stretch is calculated to shift from 888 to 815 cm^{-1} in the 19-CD_3 derivative (Table VII). Therefore, the new

Table VII. Calculated Frequencies and Assignments of CH_3 Group Vibrations of Retinal[a]

	obsd	calcd	description
unmodified	1446	1448	(20CH_3) in-plane def
		1448	(19CH_3) in-plane def
		1446	(19CH_3) out-of-plane def
		1445	(20CH_3) out-of-plane def
	1389	1388	(19CH_3) symmetric def
		1382	(20CH_3) symmetric def
		1084	0.64(19CH_3or) + 0.56(20CH_3or)
		1084	0.57(19CH_3or) – 0.63(20CH_3or)
		1022	0.55(19CH_3r) – 0.42(20CH_3r) + 0.10(8–9) – 0.08(12–13)
	1008	1015	0.54(20CH_3r) + 0.43(19CH_3r) + 0.08(8–9) + 0.12(12–13)
		888	0.21(9–CH_3) + 0.12(13–CH_3)
	866	871	0.22(13–CH_3) – 0.10(9–CH_3)
10-D	1042	1039	0.60(19CH_3r) + 0.36(10D) – 0.21(20CH_3r)
	1008	1016	0.64(20CH_3r) + 0.26(19CH_3r) + 0.14(12–13)
		873	0.25(13–CH_3)
	853	839	0.20(9–CH_3) + 0.47(10D)
11-D		1023	0.56(20CH_3r) – 0.38(19CH_3r) + 0.11(12–13) – 0.06(8–9)
	1009	1018	0.57(19CH_3r) + 0.34(20CH_3r) + 0.12(8–9) + 0.07(12–13)
		888	0.21(9–CH_3) + 0.11(13–CH_3)
	867	871	0.23(13–CH_3) – 0.10(9–CH_3)
12-D	1037	1033	0.62(20CH_3r) – 0.19(19CH_3r) + 0.11(12–13) + 0.44(12D)
	1007	1018	0.67(19CH_3r) + 0.21(20CH_3r) + 0.12(8–9)
		884	0.23(9–CH_3)
	835	825	0.20(13–CH_3) + 0.44(12D)
11,12-D_2	1036	1033	0.63(20CH_3r) – 0.15(19CH_3r) + 0.11(12–13) + 0.41(12D)
	1008	1019	0.67(19CH_3r) + 0.16(20CH_3r) + 0.13(8–9)
		884	0.23(9–CH_3)
	836	825	0.20(13–CH_3) + 0.44(12D)
10,11-D_2	1042	1038	0.58(19CH_3r) – 0.27(20CH_3r) + 0.36(10D)
	1008	1019	0.59(20CH_3r) + 0.32(19CH_3r) + 0.12(12–13)
		873	0.25(13–CH_3)
	854	839	0.20(9–CH_3) + 0.47(10D)
19-CD_3	1446	1448	(20CH_3) in-plane def
		1445	(20CH_3) out-of-plane def
	1388	1385	(20CH_3) sym def
	1079	1110	(19CD_3) sym def
		1085	0.37(20CH_3or)
		1047	(19CD_3) in-plane def
		1047	(19CD_3) out-of-plane def
	1018	1017	0.69(20CH_3r) + 0.14(12–13)
	907	867	0.53(19CD_3or)
		878	0.24(13–CH_3)
	850	850	0.53(19CD_3r)
	830	815	0.18(9–CD_3)

[a] Abbreviations used: r, in-plane methyl rock; or, out-of-plane methyl rock. Methyl deformations and rocking modes were defined as in ref 22. The deformations and out-of-plane rocks were unmixed with other vibrations in the calculations, and varied in frequency by less than 1 cm^{-1} in any of the vinyl-deuterated derivatives.

(43) Gill, D.; Kilponen, R. G.; Rimai, L. *Nature (London)* **1970**, *227*, 743.

moderately intense Raman line at 850 cm^{-1} in 19-CD_3 can reasonably be assigned to the in-plane rock shifted from 1008 cm^{-1}, and the line at 830 cm^{-1} is attributed to the C_9–CD_3 stretch shifted down from ~890 cm^{-1}. The weak line at 907 cm^{-1} can be explained as the out-of-plane rock shifted from near 1085 cm^{-1}, which derives intensity by mixing with nearby HOOP vibrations (calculated shift 1084 → 867 cm^{-1}). We are unable to explain the new line appearing at 709 cm^{-1} as either a methyl stretch or a methyl rock.

Previous workers[8a,14] have attributed the 1008-cm^{-1} Raman line to degenerate C–CH_3 stretches, although they seem not to have considered the alternative rock assignment. Since none of the earlier data included isotopic derivative spectra which could distinguish methyl rocks from methyl stretches as effectively as our spectra of deuterated retinals, we feel justified in making the above revised assignments. In 11-cis isomers the degeneracy of the methyl rocks is evidently removed, since two Raman lines are observed at 998 and 1018 cm^{-1} in 11-*cis*-retinal[44] and at 1000 and 1018 cm^{-1} in rhodopsin.[5a] The [19-CD_3]rhodopsin spectra obtained by Eyring et al.[11] permit us to assign the 1000-cm^{-1} rhodopsin line to the C_{13}–CH_3 rock and the 1018-cm^{-1} line to the C_9–CH_3 rock. The C_9–CH_3 rock in rhodopsin thus appears at a "normal" isolated rock frequency (~1018 cm^{-1}), while the C_{13}–CH_3 rock is at lower frequency. As suggested by Callender et al.,[44] it is reasonable to conclude that this low rock frequency is due to steric interactions between the $C_{20}H_3$ group and the C_{10} hydrogen in an 11-cis,12-s-trans chromophore.

Finally, it should be noted that the absence of large changes between 1100 and 1360 cm^{-1} in the 19-CD_3 spectrum (Figure 6) demonstrates that none of the intense fingerprint lines involves significant motion of $C_{19}H_3$ hydrogens. The earlier attribution of a substantial degree of $C_{19}H_3$ rocking character to the intense 1197-cm^{-1} line[8b] is therefore incorrect.

Ionyl Ring Vibrations

We attribute several bands in the retinal spectra to vibrations of the β-ionyl ring because of their insensitivity to chain deuteration, and because they correspond to lines in the Raman or IR spectra of β-ionone.[8b,23] The Raman spectrum of β-ionone shows intense polarized lines at 584, 790, 1123, 1139, and 1254 cm^{-1}, and weaker lines at 1044 and 1064 cm^{-1}. *all-trans*-Retinal has IR bands or weak Raman lines within 5 cm^{-1} of each of these frequencies which are nearly unchanged in frequency or intensity in our deuterated and demethyl derivatives. Further evidence supporting the assignment of the weak retinal Raman lines at 584, 792, 1045, 1065, and 1260 cm^{-1} to vibrations localized on the ring is provided by the spectra of 9-*cis*-, 11-*cis*-, and 13-*cis*-retinal,[8b,23] all of which have corresponding weak lines. The moderately intense IR absorptions near 1123 and 1134 cm^{-1} in all of our all-trans derivatives (Figure 2A–F) also appear in the IR spectra of other retinal isomers, and are insensitive to chain deuteration or to removal of methyl groups. We therefore also attribute these lines to ring vibrations.

Protonated Schiff Bases and Pigments

Now that we have assigned the major Raman lines and developed a force field for *all-trans*-retinal, it is important to discuss the changes in the vibrational spectra which would be expected for retinal-containing pigments. Schiff base formation should only moderately perturb the vibrational spectrum of retinal, since it adds no new internal coordinates and does not greatly alter the ground-state electronic structure. It is therefore not surprising that the Raman spectrum of the *all-trans*-retinal Schiff base[5c] is very similar to that of the aldehyde. The only significant differences are the appearance of a shoulder at 1154 cm^{-1} and the upshift of the C_{10}–C_{11} stretch to 1178 cm^{-1}. These observations can be explained if Schiff base formation causes the 1111-cm^{-1} C_{14}–C_{15} stretch of the aldehyde to shift up to ~1154 cm^{-1}, where it mixes with the nearby C_{10}–C_{11} stretch. The observed sensitivity of the 1154- and 1178-cm^{-1} lines of the Schiff base to 15-D substitution[5c] is consistent with this assignment.

Protonation of the Schiff base adds new NH rocking, wagging, and stretching coordinates, as well as significantly altering the π-electron distribution along the chain. Our QCFF-π calculations on retinal aldehydes and PSB's predict major perturbations of the $C_{14}H$, $C_{15}H$, and NH rocks and HOOPs and of the C_{14}—C_{15} and C_{15}=N stretches, as well as reduction of the C=C stretching frequencies. Nevertheless, the RR spectrum of *all-trans*-retinal PSB[5a] is quite similar to that of the aldehyde. The 1165- and 1198-cm^{-1} lines of the PSB, although their relative intensities differ, correlate with the 1163- and 1197-cm^{-1} lines of the aldehyde, and can thus be assigned to the C_{10}–C_{11} and to the presumably unresolved C_8–C_9 and C_{12}–C_{13} stretches, respectively. The 1270-cm^{-1} line, which we have assigned to the $C_{11}H$ rock, appears also in the RR spectrum of the PSB, as do the ~967-cm^{-1} A_u HOOPs and the 1008-cm^{-1} CH_3 rocking mode. The only major differences in the PSB spectrum[5a] are the disappearance of the 1334-cm^{-1} $C_{14}H$ rocking vibration, and the appearance of a new line at 1240 cm^{-1}, which corresponds to the 1253-cm^{-1} line observed in bacteriorhodopsin.[5c] This line is the only major line in the fingerprint whose frequency is sensitive to C_{15} deuteration,[5c] and it is thus localized near the Schiff base. The 1240-cm^{-1} line of *all-trans*-retinal PSB appears to shift to 1271 cm^{-1} in the 15-D derivative, paralleling the shift of the 1253-cm^{-1} line of bacteriorhodopsin to 1271 cm^{-1}.[5c] These shifts are similar to the 37-cm^{-1} upshift observed for the C_{14}–C_{15} stretch of the aldehyde upon 15-D substitution, and it therefore seems reasonable to suggest that the 1240-cm^{-1} line of the PSB is predominantly the C_{14}–C_{15} stretch. The increased frequency of the C_{14}–C_{15} stretch in the PSB compared to that of the aldehyde is consistent with the increased π-electron delocalization, which should increase the C_{14}–C_{15} ground-state bond order. The fact that this line shifts up when C_{15} is deuterated demonstrates that the $C_{15}H$ rock of the PSB is above 1240 cm^{-1}. Also, as has been discussed by Stockburger, the sensitivity of the 1240-cm^{-1} line to 15-D substitution indicates that the C_{14}–C_{15} stretch must be strongly coupled with the $C_{15}H$ rock.[45,46]

Correlations of pigment spectra with aldehyde spectra can be made quantitative by refining the molecular force field to fit observed spectra of pigment derivatives. We have previously carried out such an analysis of the HOOP vibrations of the primary visual photoproduct, bathorhodopsin.[13] The changes in the out-of-plane force constants which were required to reproduce the frequencies of deuterated derivatives of bathorhodopsin provided evidence for localized interactions between opsin and the chromophore. A similar analysis of the conformationally sensitive skeletal vibrations of rhodopsin and bacteriorhodopsin should furnish even more specific information about chromophore–protein interactions that are important for the function of these pigments.

Acknowledgment. We wish to thank I. Palings and R. Fransen for their work on the synthesis of [19-CD_3]retinal. Demethylretinoic acids from Hoffmann-La Roche were generously provided by Dr. L. Stryer. We are grateful to M. Stockburger for communicating his manuscript on bacteriorhodopsin prior to publication. This work was supported by the National Science Foundation (CHE 81-16042) and by the National Institutes of Health (EY-02051). R.M. is an Alfred P. Sloan Research Fellow (1979–1981) and an NIH Research Career Development Awardee (EY-00219).

Registry No. A, 116-31-4; B, 74352-10-6; C, 77871-13-7; D, 77871-14-8; E, 74352-09-3; F, 82178-69-6; 15-monodeuterio-*all-trans*-retinal, 75238-14-1; 9-demethyl-*all-trans*-retinal, 24336-19-4; 13-demethyl-*all-trans*-retinal, 24336-20-7; 19-trideuterio-*all-trans*-retinal, 77287-25-3.

Supplementary Material Available: The Cartesian coordinates used in the calculations and a complete description of the force field will be found in Tables VIII and IX (5 pages). Ordering information is given on any current masthead page.

(44) Callender, R. H.; Doukas, A.; Crouch, R.; Nakanishi, K. *Biochemistry* **1976**, *15*, 1621.

(45) Alshuth, Th.; Stockburger, M. *Ber. Bunsenges. Phys. Chem.* **1981**, *85*, 484.

(46) Massig, G.; Stockburger, M.; Gärtner, W.; Oesterhelt, D.; Towner, P. *J. Raman Spectrosc.* **1982**, *12*, 287.